Disruption of place cell remapping by scopolamine during aversive learning

Garrett J. Blair[1], Changliang Guo[2,3,4], Michael S. Fanselow[1,4], Peyman Golshani[2,3,4], Daniel Aharoni[2,3,4], Hugh T. Blair[1,4]

[1]Department of Psychology, UCLA, Los Angeles, CA 90095-1563, USA.

[2]David Geffen School of Medicine, University of California Los Angeles, Los Angeles, CA, 90095 USA

[3]Department of Neurology, David Geffen School of Medicine, University of California, Los Angeles, Los Angeles, CA, USA

[4]Integrative Center for Learning and Memory, University of California, Los Angeles, Los Angeles, CA, USA

ABSTRACT. We performed *in-vivo* calcium imaging of hippocampal place cells in freely behaving rats (n=14) to investigate whether the muscarinic acetylcholine receptor (mAChR) antagonist scopolamine, which is known to impair aversive learning, also disrupts place cell remapping that occurs during such learning. CA1 neurons were imaged using a large-field-of view version of the UCLA miniscope (MiniLFOV) while rats performed a shock avoidance task on a rectangular maze. Drug-free avoidance training and extinction caused place cells to remap near the shocked location, in accordance with prior studies. Systemic pre-training injections of scopolamine (1 mg/kg) did not impair immediate shock avoidance, and also did not disrupt spatial tuning properties or shock-evoked responses of place cells during training. However, the drug impaired 48 h retention of avoidance and also prevented place cells from remapping near the shocked location. In addition, when rats navigated the maze on scopolamine, CA1 population vectors showed degraded between-session similarity with drug-free maze visits on prior days, suggesting that mAChR antagonism acutely degraded the fidelity with which stored hippocampal representations were retrieved. Based upon these results, we propose that scopolamine causes amnesia by degrading the dynamics of hippocampal memory retrieval at the population level, thereby shielding stored memory representations from being modified by experience to encode new memories of events that occur under the influence of the drug.

INTRODUCTION

The rodent hippocampus contains place cells that fire selectively at preferred locations in space (O'Keefe and Dostrovsky, 1971). Place cells often retain stable positional tuning across repeated visits to the same environment (J. K. Leutgeb et al., 2005; Lever et al., 2002), but can also change their firing properties with the passage of time (Cai et al., 2016; Keinath et al., 2022; Kinsky et al., 2018; Mankin et al., 2012; Ziv et al., 2013) or in response to behaviorally significant events (Alvernhe et al., 2011; Bostock et al., 1991; Colgin et al., 2008; S. Leutgeb et al., 2005; Moita et al., 2004; Wang et al., 2015). Such "remapping" by place cells may enable them to encode information not just about the animal's present location in space, but also about past experiences that have occurred there (Cai et al., 2016; Colgin et al., 2008; S. Leutgeb et al., 2005) or future events that can be expected to occur there (Miller et al., 2017; Stachenfeld et al., 2017). By binding information about events to representations of the locations where the events occur, place cell remapping may play an important role in hippocampal processing that underlies storage and retrieval of episodic memories (Colgin et al., 2008; Josselyn and Tonegawa, 2020; S. Leutgeb et al., 2005; Mau et al., 2020).

Acetylcholine (ACh) projections to the hippocampus are thought to be important for regulating memory (Frotscher and Misgeld, 1989; Green et al., 2005; Hasselmo, 2006). Drugs that block ACh receptors have been found to impair hippocampal memory processing (Anagnostaras et al., 1999, 1995; Atri et al., 2004; Decker et al., 1990; Green et al., 2005; Hasselmo and McGaughy, 2004; Huang et al., 2011; Solari and Hangya, 2018), whereas drugs that upregulate ACh neurotransmission can facilitate learning and memory (Barten and Albright, 2008; Digby et al., 2010; Ragozzino et al., 2012) and are commonly prescribed to treat aging-related amnesia and dementia in human patients (Lombardo and Maskos, 2015). Rodent models have been utilized to investigate how ACh acutely influences neural activity in the hippocampus, including the activity of place cells. Stimulating cholinergic inputs to the

hippocampus alters EEG states by promoting theta oscillations and suppressing sharp-wave ripples (Hunt et al., 2018; Jarzebowski et al., 2021; Ma et al., 2020; Vandecasteele et al., 2014; Zylla et al., 2013). ACh antagonists have been reported in some studies to degrade the spatial tuning of place cells (Brazhnik et al., 2004; Sun et al., 2021), whereas other studies report that ACh antagonists primarily alter temporal (rather than spatial) firing properties, such as synchronization with hippocampal theta rhythm (Douchamps et al., 2013; Newman et al., 2017). ACh antagonists interfere with the ability of place cells to form and update spatial maps across repeated visits to the same environment (Douchamps et al., 2013), suggesting a potential role for ACh in place cell remapping (for a full review, see Dannenberg et al., 2017). However, it is not known whether ACh transmission is necessary for environmental events to induce place cell remapping, or whether ACh antagonist drugs might produce their amnesic effects by disrupting place cell remapping.

To investigate these questions, we performed *in vivo* calcium imaging of place cells in the CA1 layer of the rat hippocampus during an aversive shock avoidance learning task. Place cell remapping has been shown to occur at locations where animals experience aversive events such as shocks, predator odors, or attacks (Kim et al., 2015; Moita et al., 2004, 2003; Schuette et al., 2020; Wang et al., 2015, 2012). Replicating these prior studies, we observed that in drug-free rats, avoidance learning caused place cells to remap at the location where shock was encountered. Systemic pre-training injections of the muscarinic ACh receptor (mAChR) antagonist scopolamine (1 mg/kg) blocked this place cell remapping without impairing spatial tuning properties or shock-evoked responses of place cells. As in prior studies (Anagnostaras et al., 1999, 1995; Decker et al., 1990; Green et al., 2005; Huang et al., 2011; Wallenstein and Vago, 2001), scopolamine also impaired long-term retention of avoidance learning. When rats navigated the maze on scopolamine, CA1 population vectors showed degraded between-session similarity with prior (drug-free) maze visits. These findings show for the first time that impairment of aversive learning by scopolamine is accompanied by impairment of

place cell remapping in the hippocampus. We discuss the implications of these findings for understanding how cholinergic neurotransmission and place cell remapping contribute to hippocampal information processing that supports learning and memory.

RESULTS

Male (n=7) and female (n=8) Long-Evans rats underwent survival surgery to inject 1.2 uL of AAV9-Syn-GCamp7s (*AddGene*) in the hippocampal CA1 layer; ~2 weeks later, a 1.8 mm diameter GRIN lens stack (~0.5 pitch) was unilaterally implanted to image CA1 (Supplementary Fig. 1). A baseplate was attached to the skull for mounting the miniscope, and then rats began a regimen of running one 15 m session per 48 h on a 250x125 cm rectangular maze (Fig. 1A). Rats earned 20 mg chocolate pellets by alternating between two rewarded corners. On each trial, rats were free to choose a direct short path (250 cm) or an indirect long path (500 cm) to reach the next reward. During early sessions, rats learned to prefer the short over the long path (Fig. 1C,D). Upon reaching criterion for short path preference, rats began receiving drug-free shock, scopolamine shock, or barrier training sessions (Fig. 1B).

Scopolamine impairs avoidance learning

During shock training sessions (drug-free or scopolamine), rats performed the standard alternation task for 10 m. Then a 1.0 mA scrambled current was switched on to electrify grid bars in a 50 cm segment of the short path's center (Fig. 1A). Identical grid bars spanned the full length of the long and short paths, so there were no local cues to indicate the shock zone's location. After encountering the shock zone 1-2 times, rats subsequently avoided the short path during the final 5 m of the session (Fig. 1E). In the scopolamine shock condition, rats received 1.0 mg/kg scopolamine via intraperitoneal injection 30 min prior to the start of the shock

session. In the barrier control condition, the maze was not electrified; instead, a clear plexiglass barrier was placed in the center of the short path, forcing the rat to take the long path during the final 5 m of the session.

During the first 10m of training on scopolamine (before shock delivery), 6/10 rats (3M, 3F) fell below criterion for preferring the short path (compared with 0/14 drug-free rats). These rats earned a median of 5 short path rewards/m during the drug-free session given 48 h before training, but only 1.9 short path rewards/m during the first 10 m (before shock) of their training session on scopolamine (Wilcoxon test, p=.0098). Thus, prior to shock delivery, scopolamine impaired expression of the rats' learned preference for taking the short path (Fig. 1E, middle).

During the training session, rats earned fewer rewards/m on the short path after than before grid electrification (Fig. 1F) in both the drug-free (n=14, signed-rank test, $p=1.2e^{-4}$) and scopolamine (n=10, signed-rank test, p=.004) conditions. Rats in the barrier condition (n=6) were likewise forced to stop taking the short path after it was blocked by the barrier (Fig. 1F, left panel). Rats in the drug-free shock condition showed long-term retention of avoidance (Fig. 1G, left), earning fewer rewards/m on the short path 48 h after than 48 h before training (Fig. 1H, Wilcoxon test, $p=3.7e^{-4}$). By contrast, most rats trained on scopolamine showed similar short path reward rates during drug-free sessions given 48 h before and after training (Fig. 1H, Wilcoxon test, p=.125), and thus failed to exhibit long-term retention of avoidance (Fig. 1G, middle). When tested 48 h after training, rats shocked on scopolamine showed less avoidance of the short path than rats shocked drug-free (rank sum test: p=.0235; Fig. 1H). Hence, pre-training scopolamine injections impaired aversive learning, consistent with prior studies (Anagnostaras et al., 1995; Decker et al., 1990; Green et al., 2005). There was no difference in acquisition of avoidance between male versus female rats in the drug free or scopolamine shock conditions (Supplementary Fig. 8A). After shock avoidance training, rats continued to run standard sessions on the maze every 48 h until they reached the avoidance extinction criterion (Fig. 1J). Rats in the barrier control condition did not avoid the short path after training (Fig. 1H),

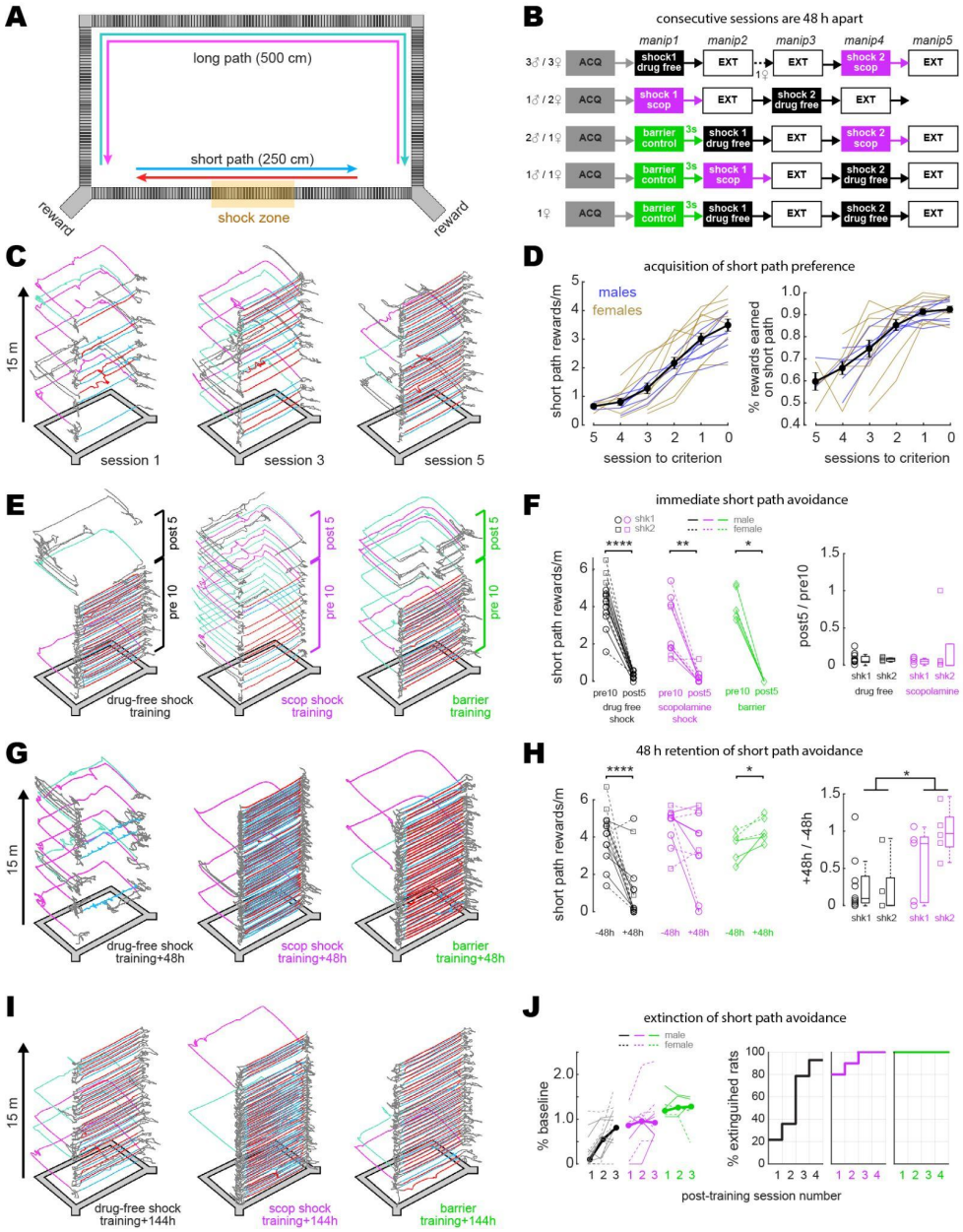

Figure 1. Disruption of aversive avoidance acquisition by scopolamine. A) Overhead view of the rectangular maze. B) Order of treatment for 5 subgroups of rats in the study. C) Example trajectories from sessions 1, 3, & 5 during initial acquisition of short path preference. D) Acquisition curves for short path preference; criterion was reached on session 0. E) Example maze trajectories from training sessions. F) Left: Rewards/m earned on the short path during the first 10 m (pre10) versus last 5 m (post5) of training sessions; symbols indicate whether each rat received its first (shk1) or second (shk2) shock during a session. Right: Box plots show post-shock reduction in short path rewards/m (post5/pre10). G) Example maze trajectories 48 h after training. H) Left: Rewards/m earned on the short path during drug-free sessions given 48 h before (-48h) vs. after (+48h) training. Right: Box plots show 48 h retention of shock avoidance (+48h / -48h). I) Example maze trajectories 144 h after training. J) Left: Extinction curves over the first 3 post-extinction sessions; short path preference is measured relative to baseline 48 h before training (thin lines: individual rats, thick lines: per session median). Right: Cumulative distributions show percentage of rats in each training condition meeting extinction criterion (≥2 rewards/m on the short path, and at least twice as many short path rewards as long path rewards) at 1, 2, 3, or 4-days after training. *p<.05, **p<.01, ****p<.0001.

but instead increased their preference for the short path (Mann-Whitney U test, p=.0313), presumably because they continued to acquire a greater preference for the short path during barrier training.

Scopolamine disrupts between- but not within-session place cell stability

A large-field-of view version of the UCLA Miniscope (Cai et al., 2016; Guo et al., 2021) (MiniLFOV) was used to image neurons in the hippocampal CA1 layer during maze sessions (Fig. 2A). Calcium activity was analyzed only during traversals of the short path, since the long path was undersampled after rats had learned to prefer the short path. Analysis was further restricted to *beeline trials* during which the rat ran directly from one reward zone to the other on the short path, without any pause or change in direction (Fig. 2B; Supplementary Video 1); this assured that imaging data came from periods of active locomotion when place cells exhibit reliable spatial tuning, and that the rats' behavior during imaging was similar across all experimental sessions and conditions. To further control for possible confounding effects of behavior differences between sessions (Supplementary Fig. 2), beeline trials were randomly subsampled using an algorithm (see Methods) that minimized trial count and running speed differences between the drug-free and scopolamine conditions (Fig. 2C). Spatial tuning was then analyzed and compared during these behaviorally homogeneous trials.

To analyze spatial tuning, the short path was subdivided into 23 spatial bins (each 10.8 cm wide). Two spatial tuning curves (one per running direction) were derived for each neuron. Cell activity was measured in units of *active frames per second* (Af/s), defined as the mean number of imaging frames per second during which a neuron generated at least one inferred spike. A neuron was classified as a place cell if its LR or RL tuning curve (or both) met defined criteria for minimum Af/s, spatial selectivity, and spatial stability within a session (see Methods).

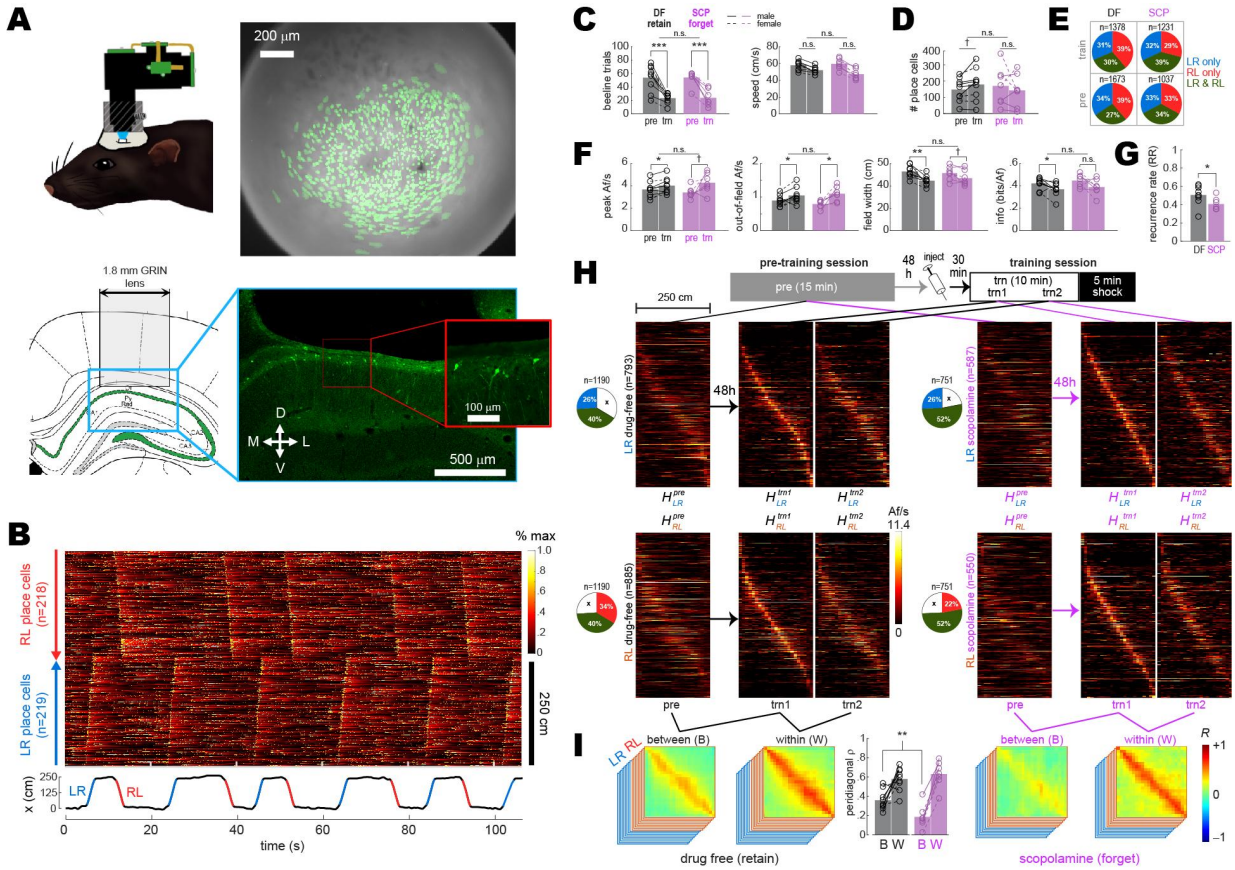

Figure 2. *Scopolamine impairs between- but not within-session population coding.* A) *Upper left*: Illustration of rat wearing MiniLFOV. *Upper right*: Cell contours identified during a single example session in one rat. *Lower left*: Target position of GRIN lens over the CA1 layer. *Lower right*: Fluorescence image of lens position from the example rat. B) *Top*: Rastergram shows normalized calcium fluorescence traces of place cells (one per row, sorted by preferred firing location and direction) during several traversals of the short path. *Bottom*: Rat's position (black) with running epochs colored by direction of travel ("LR", left to right, in blue; "RL", right to left, in red). C) Individual rat data (lines & symbols) and session means (bars) for the number of subsampled beeline trials (left) and median beeline running speed (right) during pre-training (*pre*) and training (*trn*) sessions; subsampled beeline trial counts were lower for *trn* than *pre* sessions because only trials from the first 10 min of *trn* (prior to shock delivery) were included; running speeds were lower for *trn* than *pre* sessions because scopolamine (SCP) reduced running speeds, resulting in preferential subsampling of slower beeline trials from drug-free (DF) sessions by the algorithm that minimized running speed differences between training conditions (see Methods). D) Bar/line graph shows number of place cells imaged per rat during *pre* and *trn* sessions. E) Pie graphs show percentages of place cells imaged per condition ('n' gives total number summed over rats) that were spatially tuned in the LR only, RL only, or both LR&RL running directions. F) Tuning curve properties of place cells imaged during *pre* and *trn* sessions. G) Place cell recurrence ratios (RR) between *pre* and *trn* sessions. H) *Top*: Diagram shows timeline for *pre* and *trn* sessions given 48 h apart. *Bottom:* Tuning curve heatmaps for recurring place cells (from all rats combined, co-sorted by peak locations from the *trn1* session) that were spatially tuned in the LR (top) or RL (bottom) running directions; separate heatmaps are shown for *pre*, *trn* part one (*trn1*), and *trn* part two (*trn2*) sessions. I) Between- (B) and within- (W) session population vector correlation matrices are shown for DF and SCP shock training conditions; middle bar graph shows median peridiagonal correlation value (ρ) for each rat (lines & symbols) and mean over rats (bars) for B and W heatmap pairs. Asterisks in 'C' and 'D' denote significance for main effect of DF vs. SCP or uncorrected t-test comparing *pre* vs. *trn* sessions; asterisks in 'E' and 'G' denote significance for uncorrected t-tests. † p<.1; *p<.05; **p<.01; ***p<.001.

About 1/3 of place cell tuning curves met criteria for spatial selectivity only in the LR direction, 1/3 only in the RL direction, and 1/3 in both directions (Fig. 2E).

To analyze acute effects of scopolamine on CA1 place cell activity, data from shock training sessions given drug-free or on scopolamine was compared against data from pre-training baseline sessions (always drug-free) given 48 h earlier. The drug-free condition only included rats (n=9) that retained avoidance of the short path 48 h after shock training, whereas the scopolamine condition only included rats (n=7) that failed to avoid the short path 48 h after shock training (indicating that the drug had blocked avoidance learning; see Methods). A 2x2 ANOVA on the number of place cells detected per session (Fig. 2D) found no effect of training condition ($F_{1,14}$=.03, p=.87) or session ($F_{1,14}$=.014, p=.9), and no interaction ($F_{1,14}$=2.1, p=.17).

Four properties of spatial tuning curves were analyzed: peak Af/s rate, out-of-field Af/s rate, tuning width, and spatial information content (see Methods). For each rat and each session, median values of these tuning properties were taken over all LR and RL tuning curves that met spatial selectivity criteria (Supplementary Fig. 3); 2x2 mixed ANOVAs were then performed on the resulting rat medians for each of the four tuning properties (Fig. 2F). There were large main effects of session (pre-training vs. training) for all four tuning properties, which were driven by correspondingly large differences in behavior sampling and running speed (Fig. 2C). However, there were no main effects of training condition (drug-free vs. scopolamine) or interactions between training condition and session (Fig. 2F), indicating that none of the four tuning properties differed during training sessions given drug-free versus on scopolamine.

The *place field recurrence ratio* was defined as $RR = N_R/N_T$, where N_R is the number of place fields that recurred during the pre-training and training sessions, and N_T is the total number of recurring and non-recurring place fields detected during both sessions combined (see Methods). Mean RR values were lower (independent $t_{14} = 2.15,\ p = .0497$) during scopolamine (40.7±8.8%) than drug-free (50.7±3.9%) training sessions. To investigate how

scopolamine affected population coding by recurring place cells, two heatmaps (one per running direction, denoted H_{LR}^{pre} and H_{RL}^{pre}) were created from pre-training tuning curves of recurring place cells (Fig. 2H; Supplementary Fig. 4). Additionally, two heatmaps per running direction were created from data collected during the the first (H_{LR}^{trn1}, H_{RL}^{trn1}) and second (H_{LR}^{trn2}, H_{RL}^{trn2}) half of each training session's subsampled beeline trials, all of which occurred prior to shock delivery. Between-session population vector correlation matrices (one per running direction) were derived for each rat (Supplementary Fig. 4) with matrix entries given by $\rho_{i,j}^{btwn} = R(H_i^{pre}, H_j^{trn1})$, where H_i^{pre} and H_j^{trn1} denote population vectors in columns *i* and *j* of the pre-training and trn1 heatmaps, respectively, and R is the Pearson correlation coefficient. Within-session population vector correlation matrices were derived in a similar manner with matrix entries given by $\rho_{i,j}^{wthn} = R(H_i^{trn1}, H_j^{trn2})$, where H_i^{trn1} and H_j^{trn2} denote population vectors in columns *i* and *j* of the trn1 and trn2 heatmaps, respectively.

When population vector correlation matrices were averaged together across running directions and rats (Fig. 2I), high mean ρ^{wthn} values were observed along diagonals of within-session correlation matrices for both the drug-free and scopolamine conditions. By contrast, lower mean ρ^{btwn} values were observed along diagonals of between-session correlation matrices, in accordance with prior studies showing that place cell population vectors become decorrelated over time (Cai et al., 2016; Keinath et al., 2022; Mankin et al., 2012; Ziv et al., 2013). To quantify this decorrelation, a population vector stability score (*S*) was derived for each rat by taking the median ρ value over *K* peri-diagonal bins (see Methods) in the rat's LR and RL correlation matrices: $S = median(\rho_1^{LR}, \rho_2^{LR}, \ldots, \rho_K^{LR}, \rho_1^{RL}, \rho_2^{RL}, \ldots, \rho_K^{RL})$. A 2x2 mixed ANOVA on *S* scores with training condition (drug-free vs. scopolamine) as an independent factor and time interval (between vs. within session) as a repeated factor found no main effect of training

condition ($F_{1,14}$=1.73, p=.21), but there was a large main effect of time interval ($F_{1,14}$=71.5, p=7.1e^{-7}) and a significant interaction ($F_{1,14}$=8.05, p=.0132). Uncorrected post-hoc comparisons confirmed that this was because scopolamine injections reduced between- (t_{14}=3.07, S_{DF}<S_{SCP} p=.0084) but not within- (t_{14}=.83, S_{DF}<S_{SCP} p=.42) session population vector correlations (Fig. 2I, center). Hence, even though scopolamine did not acutely disrupt spatial tuning of CA1 neurons (Fig. 2F), the drug reduced the percentage of recurring place cells and significantly degraded the between-session (but not within-session) similarity of recurring place cell population vectors (Fig. 2H,I). Similar disruption of between- but not within-session place cell stability has been previously reported in aged rats (Barnes et al., 1997) (see Discussion).

Scopolamine caused similar disruption of between-session place cell stability in male and female rats (Supplementary Fig. 8). When analyses of Fig. 2 were repeated on scopolamine rats (n=2) that retained avoidance despite the injection, population vector similarity was not degraded between pre-training and training sessions, suggesting that impairment of between-session population vector stability was related to impairment of avoidance learning (Supplementary Fig. 5).

Scopolamine impairs aversively induced remapping

Training-induced place cell remapping was analyzed in the same subset of rats shown in Fig. 2. To measure remapping, post-extinction CA1 population vectors were compared against the 48 h pre-training baseline session. For the drug-free shock condition, post-extinction population vectors were sampled from the first session after shock training during which the rat met criterion for extinction of short path avoidance (Fig. 3A, left); this was the earliest post-training session with adequate sampling of the short path. For the scopolamine shock condition, post-extinction population vectors were sampled from the session given 8 d (that is, 4 sessions including the training session) after the pre-training session (Fig. 3A, center); this

matched the modal intersession interval for the drug-free condition, so that confounds would not arise from measuring remapping across different time intervals for the drug-free versus scopolamine conditions. Likewise, for the barrier control condition, post-extinction population vectors were also sampled 8 d after the pre-training session; one barrier training rat became startled due to external factors and stopped running early in the 8 d post-training session, so the 6 d session was used instead (Fig. 3A, right).

To control for potential confounds from between-session behavior differences (Supplementary Fig. 2), beeline trials were subsampled using an algorithm (see Methods) that equalized the number of trials from pre- and post-extinction sessions in each rat (Fig. 3B, left), while also minimizing running speed differences between sessions and training conditions (Fig. 3B). Spatial tuning was analyzed during subsampled trials, and a 3x2 mixed ANOVA on the number of place cells detected during each session (Fig. 3C, left) yielded no effect of training condition ($F_{2,19}$=.43, p=.66) or session ($F_{1,19}$=.01, p=.92), and no interaction effect ($F_{2,19}$=1.57, p=.24). The place field recurrence ratio (RR) between pre- and post-extinction sessions also did not differ among training conditions (Fig. 3C, right; one-way ANOVA: $F_{2,19} = .65,\ p = .53$).

Place cells can respond to aversive shocks by remapping their firing fields near “unsafe” locations where shocks have occurred(Moita et al., 2004, 2003; Schuette et al., 2020; Wang et al., 2012). To investigate whether such shock-induced remapping occurred in our experiment, a pair of heatmaps (pre- and post-extinction) was created from tuning curves of recurring place cells in each running direction (LR and RL) for each training condition (Fig. 3D). As in prior studies (Ziv et al., 2013), place fields tended to be more densely concentrated near the ends of the short path than in the middle (Fig. 3E). Heatmap pairs were used to derive two population vector correlation matrices per rat, P_{LR} and P_{RL} (Supplementary Fig. 6). When P_{LR} and P_{RL} were averaged across rats, a gap of low correlation appeared in the center of the diagonal for the drug-free shock condition (Fig. 3F, left) which was not seen in the scopolamine shock (Fig. 3F,

middle) or barrier (Fig. 3F, right) conditions, suggesting that drug-free shock (but not scopolamine shock or barrier) training induced remapping in the center of the short path where shock had occurred (Moita et al., 2004, 2003; Schuette et al., 2020; Wang et al., 2012).

To statistically analyze this remapping effect, template masks (Fig. 3H, right column) were used to select subsets of peri-diagonal ρ bins in three different zones of the short path: left-side zone (L), center zone (C), and right-side zone (R). For each rat, a population vector stability score was derived in each zone (S_L, S_C, S_R) by taking the median ρ value over *K* bins selected by the zone's template mask in LR and RL correlation matrices combined: *S*=*median*(ρ_1^{LR},ρ_2^{LR},...,ρ_K^{LR},ρ_1^{RL},ρ_2^{RL},...,ρ_K^{RL}). Boxplots in Fig. 3H show each rat's median and range of ρ values from bins selected by L, C, and R templates. Bar graphs (Fig. 3H, left) show means of *S* scores in the left ($\overline{S}_L$), center ($\overline{S}_C$), and right ($\overline{S}_R$) track zone for each training condition . In the center zone, $\overline{S}_C$ differed significantly between drug-free, scopolamine, and barrier conditions (one-way ANOVA: $F_{2,19} = 13.6,\ p = .0002$); uncorrected post-hoc t-tests confirmed that this was because $\overline{S}_C$ was lower in the drug-free shock than scopolamine shock ($t_{14} = 4.7,\ p = .0003$) or barrier ($t_{13} = 3.6,\ p = .0031$) conditions, which did not differ from one another ($t_{11} = .68,\ p = .51$). $\overline{S}_L$ also differed among training conditions ($F_{2,19} = 5.5,\ p = .0131$) whereas $\overline{S}_R$ differed only marginally ($F_{2,19} = 3.3,\ p = .058$). Hence, avoidance training and extinction induced more place cell remapping in the drug-free shock condition than the scopolamine shock or barrier training conditions; this remapping was more pronounced in the "unsafe" center zone where shocks occurred than in "safer" zones at L and R ends of the track where no shocks occurred. Kalmagorov-Smirnov tests found that place field density distributions (accumulated over all rats) did not change significantly between the pre versus post sessions in any training condition,

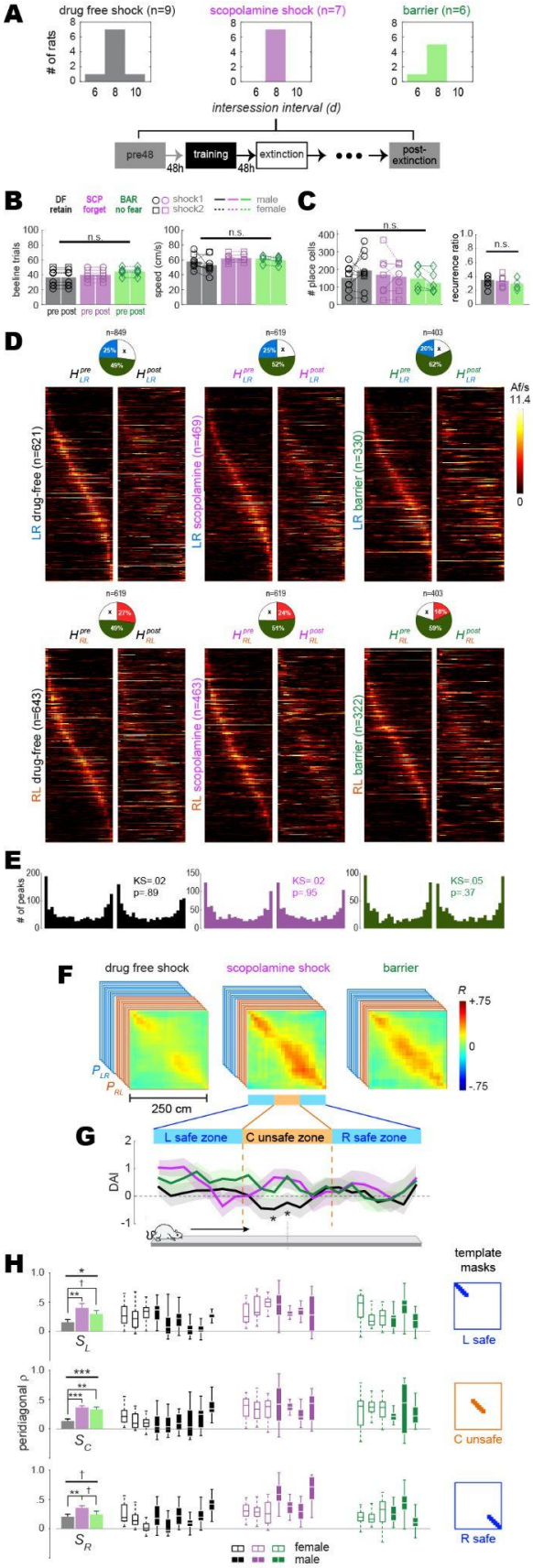

Figure 3. Scopolamine impairs shock-induced remapping of place cells. A) Top: bar graphs show distributions of intersession intervals between pre-training (pre) and post-extinction (post) session pairs included in the analysis. Bottom: Diagram shows timeline for pre and post sessions. B) Left: Number of subsampled beeline trials did not differ significantly by training condition or session. Right: Running speeds did not differ significantly by training condition; there was a marginal difference between pre vs. post running speeds in the barrier (but not drug-free or scopolamine shock) condition. C) Left: Total number of imaged place cells (recurring and non-recurring) did not differ significantly by training condition; there was a marginal difference between pre vs. post place cell counts in the barrier (but not drug-free or scopolamine shock) condition. Right: Between-session place cell recurrence ratios did not differ by training condition. D) Heatmap pairs show pre and post tuning curves for recurring place cells that were spatially tuned in the LR (top row) and RL (bottom row) running direction; both heatmaps in each pair are co-sorted by peak locations from the pre session. Pie charts show the proportion of recurring place cells (total number given at top) for which tuning curves were included in LR and RL heatmap pairs. E) Kalmagorov-Smirnov tests show that distributions of place field peaks locations (LR and RL combined) were unchanged between pre and post sessions. F) Mean population vector correlation matrices for the three training conditions. G) Decoding accuracy index (DAI) at each position on the track for each of the three training conditions; '*' indicates locations where decoding was significantly (p<.05) less accurate for the drug-free condition than the other two conditions. H) Left column: Bar graphs show means and standard errors of population vector stability scores (S); results for L, C, & R track zones are shown top, middle, and bottom rows, respectively. Middle columns: Boxplots show median and range of template-selected population vector correlation bins in each rat. Right column: Templates used to select peri-diagonal correlation values from the L, C, & R track zones.

including the drug-free shock condition (Fig. 3E, left). Hence, remapping did not result in over- or under-representation of the shock zone after extinction, in contrast with prior reports that remapping causes place fields to migrate toward locations where aversive stimuli are encountered (Mamad et al., 2019).

Induction of remapping by avoidance training and extinction did not differ in male versus female rats, nor did the impairment of remapping by scopolamine (Supplementary Fig. 8). When the analyses of Fig. 3 were repeated on scopolamine rats (n=2) that successfully retained avoidance despite the injection, the drug was less effective at inducing place cell remapping (Supplementary Fig. 7), suggesting (but not proving) that impairment of remapping was causally related to impairment of avoidance learning.

To analyze the extent of remapping caused by aversive learning, the rat's position on the track was decoded from place cell calcium activity (see Methods). The decoder was trained on data from one session (pre- or post-extinction) and tested on data from the other session. The decoding error in a given position bin was measured as the median of the absolute difference (in cm) between the rat's actual versus predicted position over all visits to that bin. Wilcoxon signed-rank tests compared decoding errors obtained with shuffled versus non-shuffled population vectors; a *decoding accuracy index* (DAI) was then derived for each bin, with DAI=0 corresponding to $p=.01$ for more accurate decoding from unshuffled than shuffled population vectors (see Methods). When mean DAI values were compared among training conditions, significant differences were detected only in two bins at the center of the track (in the shock zone) where decoding in the drug-free shock condition was significantly less accurate ($p<.05$) than in scopolamine shock and barrier training conditions combined (asterisks in Fig. 3D, bottom). In accordance with results from population vector correlation analysis, these decoding results support the conclusion that drug-free shocks induced more remapping of the center zone than shocks while on scopolamine or from barrier training.

Scopolamine does not disrupt place cell responses to shock

Shock-induced place cell remapping has been observed in prior studies (Moita et al., 2004, 2003; Schuette et al., 2020; Wang et al., 2012), but the cellular and synaptic mechanisms of such remapping are not well understood. Individual CA1 neurons can form new place fields at locations where they are artificially stimulated or inhibited (Bittner et al., 2015; Geiller et al., 2022), and since some CA1 place cells are naturally responsive to shocks (Moita et al., 2004, 2003), it is possible that individual CA1 neurons might gain or lose place fields at locations where they respond to shocks. If so, then this might partly account for remapping at the population level. If shock-evoked responses of CA1 neurons are involved in remapping, then blockade of remapping by scopolamine could be related to effects of the drug upon these shock-evoked responses. To investigate this, each place cell imaged during a training session was classified as shock responsive if its Af/s rate was significantly higher during entries to the electrified than non-electrified shock zone; otherwise, it was classified as non-responsive to shocks (see Methods).

The mean percentage of shock responsive cells per rat (Fig. 4A, left column) was 35.5±2.3% for drug-free training and 29.6±3.3% for scopolamine training; these percentages did not differ significantly (independent t_{14} =1.58; p=.13). Pre-shock baseline Af/s rates (Fig. 4A, middle column) were higher for shock responsive than non-responsive place cells in both the drug-free (t_{1931} =9.3; p<.0001) and scopolamine (t_{1034} =4.34; p<.0001) conditions, which was attributable to the fact that in both conditions, place field peaks for shock responsive and non-responsive cells tended to be segregated on the ‘approach’ and ‘departure’ sides of the shock zone, respectively (Fig. 4A, right column). Thus, as rats approached the shock zone in either running direction, shock responsive cells were more likely than non-responsive cells to be active in their place fields just before shock zone entry.

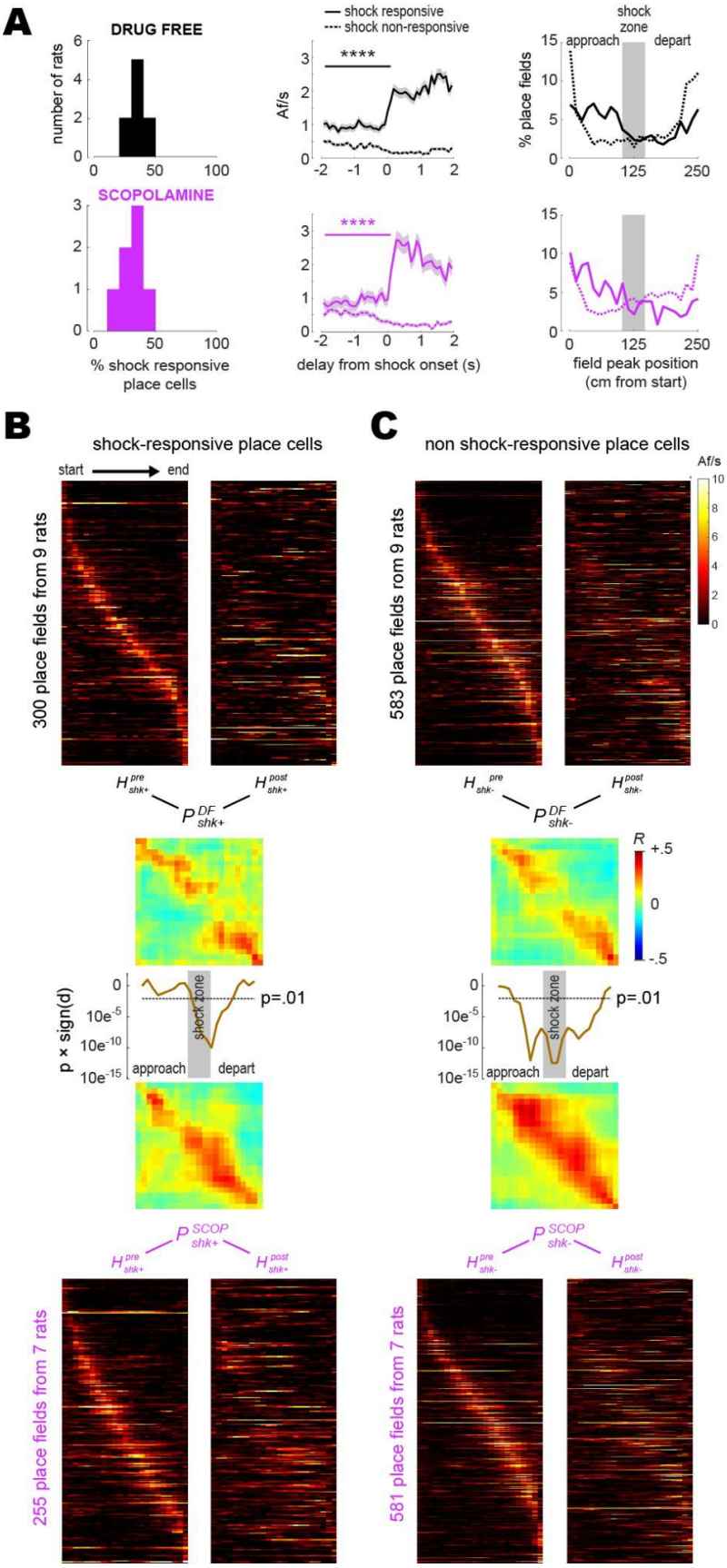

Figure 4. Scopolamine does not impair shock-evoked responses of place cells. A) Left column: Frequency distribution of shock responsive place cell percentages in each rat. Middle column: Population-averaged Af/s rates (from all rats combined) for shock responsive versus shock responsive place cells. RIght column: Spatial distribution of place field peak locations during the training session, prior to grid electrification; x-axis shows distance traveled between the start (left) and end (right) of the short path in the current running direction (LR or RL). B) Heatmaps (LR and RL tuning curves combined) are plotted for shock responsive place cells in the drug-free (top) versus scopolamine (bottom) conditions during pre- (left) and post- (right) training sessions (rows are co-sorted on peaks from the pre-training session, columns are sorted so that the rat's running direction goes from left to right for both LR and RL tuning curves); P matrices show pre- vs. post-extinction population vector correlations for shocks given drug-free (top) or on scopolamine (bottom); line graphs show that signed p-values (y-axis, log scale) fall below .01 at center track positions where drug-free shocks induced more remapping than shocks on scopolamine. C) Same as 'B' but for shock non-responsive place cells.

To compare remapping by shock responsive versus non-responsive CA1 neurons, analyses were performed on place cells that recurred during pre- and post-extinction sessions and were also active during the training session (so that each cell could be classified as responsive or non-responsive to shocks). Pre- and post-extinction heatmaps were derived from tuning curves of shock responsive (Fig. 4B) and non-responsive (Fig. 4C) place cells. LR and RL tuning curves were combined together in each heatmap, with RL (but not LR) tuning curves reflected on the horizontal so that the rat's running direction was oriented from left to right in all rows; hence, columns to the left or right of center in each heatmap denoted locations where rats were approaching or departing the shock zone, respectively. From these heatmaps, shock responsive and non-responsive population vector correlation matrices were derived for the drug-free (P^{DF}_{shk+},P^{DF}_{shk-}) and scopolamine (P^{SCOP}_{shk+},P^{SCOP}_{shk-}) conditions. A gap of low peridiagonal ρ values in the center of P^{DF}_{shk+} but not P^{SCOP}_{shk+} (Fig. 4B) and of P^{DF}_{shk-} but not P^{SCOP}_{shk-} (Fig. 4C) indicated that drug-free shocks induced remapping of the center zone in both shock responsive and non-responsive place cell populations, whereas scopolamine shocks failed to induce remapping in either population. Confirming this, a series of independent t-tests was performed on clusters of peri-diagonal bins arrayed along diagonals of P^{DF}_{shk+} versus P^{SCOP}_{shk+}, and P^{DF}_{shk-} versus P^{SCOP}_{shk-} (see Methods); resulting significance values (line graphs in Figs. 4B,C) dipped well below p<.01 in the center region of the track (but not at the ends), indicating that drug-free shocks caused shock responsive and non-responsive place cells to remap the center zone more than scopolamine shocks.

DISCUSSION

Here we found that systemic pre-training injections of scopolamine impaired acquisition of a shock avoidance task, consistent with prior reports that scopolamine disrupts aversive

learning (Anagnostaras et al., 1995; Decker et al., 1990; Green et al., 2005). We also observed that after drug-free avoidance training, hippocampal place cells remapped their firing fields at the location where shock occurred in agreement with prior findings (Kim et al., 2015; Moita et al., 2004, 2003; Schuette et al., 2020; Wang et al., 2015, 2012). Pre-training injections of scopolamine not only impaired avoidance learning but also prevented place cells from remapping in response to shock delivery, despite preserving the spatial tuning properties of place cells during the training session. This finding provides novel evidence that place cell remapping plays a role in memory encoding during aversive learning, and suggests that mAChR antagonists produce amnesia by interfering with experience-dependent plasticity of hippocampal population codes.

Implications for the role of remapping in memory

When place cells were first discovered, they were hypothesized to encode “cognitive maps” that store stable long-lasting memories of spatial environments (O’Keefe and Nadel, 1978). Supporting this, electrophysiology studies found that place cells can retain stable positional tuning across repeated visits to the same familiar environment (Lever et al., 2002). However, methodological limitations made it difficult to record large numbers of place cells over long periods of time using electrophysiology. Advances *in-vivo* calcium imaging have made it possible to perform longitudinal studies of place cell firing over days or weeks of experience. These studies show that place cells in mice (Cai et al., 2016; Keinath et al., 2022; Kinsky et al., 2018; Ziv et al., 2013) and to a lesser extent in rats (Wirtshafter and Disterhoft, 2022) can change their firing properties over time, suggesting that place cells do not merely encode spatial maps of familiar environments but may also encode mnemonic information about past experiences that have occurred in such environments (Cai et al., 2016; Colgin et al., 2008; S. Leutgeb et al., 2005; Sanders et al., 2020). If so, then when place cells remap in response to

aversive stimuli, this may help to encode new memories of when and where threatening events are encountered. Our current findings support this view by showing that when avoidance learning is impaired by scopolamine, place cell remapping is concurrently impaired as well, which may reflect a failure to store news hippocampal engrams during the aversive learning experience.

Pre-training injections of scopolamine did not impair immediate avoidance of the shocked location during the training session (Fig. 1F), consistent with prior evidence that mAChRs are not necessary for immediate shock avoidance (Decker et al., 1990). Hence, it appears that rats were still able to keep track of their own location and maintain a short-term working memory of the shocked location while on scopolamine, perhaps because place cells retained stable within-session spatial tuning (Fig. 2F-I). In contrast with our observation that spatial tuning of place cells was preserved under scopolamine in rats, a recent calcium imaging study in mice (Sun et al., 2021) reported that tuning properties of place cells on a linear track were acutely disrupted by systemic scopolamine injections at the same dosage used here (1mg/kg). This discrepancy could be due either to task differences or species differences between mice and rats (Frick et al., 2000; Stranahan, 2011), and highlights the necessity of diversity of animal models in future research (Wirtshafter and Disterhoft, 2022).

Rats that received avoidance training on scopolamine were impaired when tested for retention 48 h later (Fig. 1H), consistent with prior studies showing that mAChRs are necessary for aversive learning (Anagnostaras et al., 1999, 1995; Decker et al., 1990; Wallenstein and Vago, 2001). In conjunction with blocking avoidance learning, scopolamine also blocked place cell remapping between pre-training and post-extinction sessions (Fig. 3D-H). This suggests that scopolamine prevented the hippocampus from storing new engrams during the aversive learning experience. Prior studies have similarly shown that scopolamine interferes with the ability of place cells to form and update cognitive maps across repeated visits to the same environment (Douchamps et al., 2013), but the present study is the first to show that impairment

of behavioral learning by scopolamine is accompanied by disruption of place cell remapping that normally occurs during the course of such learning.

In our study, rats that were given drug-free avoidance training acquired and then extinguished avoidance behavior during the timespan over which remapping was measured; hence, it is difficult to dissociate whether place cell remapping was driven by acquisition, extinction, or both. Rats trained on scopolamine did not undergo extinction, since they failed to exhibit long-term retention of avoidance behavior in the first place. If remapping was driven by extinction, then scopolamine may have impaired remapping not by disrupting brain activity during the training session but instead by depriving rats of the extinction experience that would otherwise have caused remapping to occur after training. Prior evidence indicates that acquisition and extinction of conditioned fear can both contribute to place cell remapping (Moita et al., 2004; Wang et al., 2015, 2012), and place cell remapping tends to occur preferentially at locations where aversive stimuli are encountered during training (Fig. 3F-H; Fig. 4B,C; (Kim et al., 2015; Moita et al., 2004, 2003; Okada et al., 2017; Schuette et al., 2020; Wang et al., 2015, 2012); but see Okada et al., 2017). It is therefore likely that impairment of remapping by pre-training injections of scopolamine was at least partly caused by disruption of experience-dependent changes to the hippocampal population code during the training session itself.

Implications for the role of ACh in memory storage

ACh projections to the hippocampus are thought to be necessary for storing new memories of novel experiences, but may be less important for retrieving previously stored memories of familiar experiences (Green et al., 2005; Hasselmo, 2006). Supporting this view, manipulations that impair ACh neurotransmission have been found to selectively impair memory storage but not retrieval of semantic information (Atri et al., 2004; Hasselmo and McGaughy,

2004) and fear memories (Decker et al., 1990; Huang et al., 2011). Hippocampal synaptic plasticity is likewise thought to be more important for storing new memories than for retrieving old memories (Martin et al., 2000), and has been implicated in place cell remapping (Dragoi et al., 2003). Since hippocampal plasticity is sensitive to mAChR antagonists (Drever et al., 2011), it is possible that scopolamine impaired avoidance learning and place cell remapping in our study by interfering with synaptic plasticity in the hippocampus. The drug may also have impaired memory storage by interfering with plasticity in other brain regions such as the amygdala, where associations between predictive cues and noxious stimuli are thought to be stored during aversive learning (Blair et al., 2001; d'Aquin et al., 2022; Grewe et al., 2017) and are also susceptible to cholinergic modulation (Jiang et al., 2016).

Some CA1 place cells are excited by shocks (Moita et al., 2004, 2003), and it has been shown that individual CA1 neurons can form new place fields at locations where they are artificially excited or inhibited (Bittner et al., 2015; Geiller et al., 2022; McKenzie et al., 2021; Schoenenberger et al., 2016). This raises the possibility that during aversive learning, shock-evoked responses of CA1 neurons might trigger synaptic plasticity that leads to remapping. If so, then blockade of remapping by scopolamine could be caused by disruption of these shock-evoked responses that trigger plasticity. However, we found that scopolamine did not alter shock-evoked responses of place cells (Fig. 4), so if the drug impaired hippocampal plasticity, it probably did not do so by disrupting the ability of shocks to excite place cells.

Implications for the role of ACh in memory retrieval

In the present study, we did not investigate whether pre-testing scopolamine injections impaired retrieval of previously learned avoidance behavior. However, we did observe that when scopolamine was given prior to avoidance training, the drug impaired retrieval of the rats' previously learned preference for the taking short path on the rectangular maze (Fig. 1F). This

finding is consistent with prior studies showing that scopolamine can impair expression of previously learned spatial behaviors (Huang et al., 2011; Svoboda et al., 2017; Vales and Stuchlik, 2005). Moreover, while rats were on scopolamine, place cell recurrence ratios were reduced (Fig. 2G) and CA1 population vectors showed degraded between-session similarity with drug-free maze visits on prior days (Fig. 2H,I). These findings suggest that scopolamine interfered with retrieval of previously stored place cell population vectors, which in turn implies that the drug did not selectively impair memory encoding processes (such as hippocampal plasticity) while sparing memory retrieval processes. Instead, it appears that scopolamine produced a combination of interrelated effects on both encoding and retrieval.

By degrading between-session stability of place cells (Fig. 2H,I), scopolamine may have prevented CA1 networks from retrieving accurate place cell representations of the familiar maze environment during the training session, thereby 'shielding' these representations from modification (in the form of place cell remapping) by the aversive learning experience. Failure to retrieve accurate place cell representations on scopolamine may also have degraded the rats' ability to recognize the maze as the same familiar environment where they had previously learned to prefer the short path (resulting in the observed impairment of short path preference), and prevented hippocampal representations of the familiar environment from becoming associated with the aversive shock in other brain structures such as the amygdala (contributing to observed impairments of avoidance retention). It is possible that disruption of theta synchrony among place cells by scopolamine (Douchamps et al., 2013; Newman et al., 2017) may also have contributed to the drug's effects upon learning, remapping, and population vector stability. However, calcium imaging does not afford adequate time resolution for investigating contributions of theta oscillations, so we were unable to address this in the current study.

Implications for animal models of aging

Like humans, rodents show memory deficits with aging (Barnes, 1979; Barnes et al., 1980). Interestingly, prior studies have shown that place cell population dynamics in aged rats are altered in ways similar to those observed here under scopolamine. For example, we found that scopolamine degraded between- but not within-session stability of the CA1 population code (Fig. 2F-I), which has also been observed in aged rats (Barnes et al., 1997). This is in contrast to other brain diseases, such as epilepsy, which degrades both within- and between-session place coding (Shuman et al., 2020). Additionally, we found that in rats that showed impaired avoidance learning after pre-training injections of scopolamine (Fig. 1F), the drug concurrently prevented CA1 place cells from remapping during learning and extinction (Figs. 3,4). Place cells in aged rodents have likewise been reported to show deficits in experience-dependent modification of their tuning properties (Oler and Markus, 2000; Tanila et al., 2018; Wilson et al., 2004, 2003). These parallels between the effects of aging and scopolamine upon place cells suggest that mAChR blockade and aging may produce similar memory deficits by causing similar impairments to hippocampal population stability. Further study is warranted to investigate whether such impairments of hippocampal population coding can be reversed using anti-amnesic drugs, such as those that upregulate ACh transmission or other novel compounds. By identifying interventions that can improve the long-term stability of hippocampal population coding in animal models, it may be possible to make progress toward improved therapies for memory deficits associated with aging and neurodegenerative disease.

ACKNOWLEDGEMENTS

We thank Dr. Andrew Howe, Shiyun Wang, Ryan Grgurich, and Umais Khan for helpful comments on the experimental design and manuscript. This work was supported by NSF NeuroNex 1704708 (HTB, PG, DA) and RO1-MH062122 (MSF).

METHODS

All experimental procedures were approved by the Chancellor's Animal Research Committee of the University of California, Los Angeles, in accordance with the US National Institutes of Health (NIH) guidelines. Raw data files and analysis code are openly available at https://github.com/tadblair/tadblair/tree/Blair_et_al.

Subjects

15 Long Evans rats (8F, 7M) acquired from Charles River at 3 months of age were used in this experiment. Subjects were singly-housed within a temperature and humidity controlled vivarium on a 12 hour reverse light-cycle. Surgical procedures began after a one week acclimation period in the vivarium, and recordings and behavioral experiments began around 5 months of age. Fig. 1B shows the order in which experimental manipulations were given to different groups of rats. 6 rats (3 male, 3 female) received drug-free shock training as their first manipulation after reaching criterion for preferring the short path. Of these, 5 rats (3 male, 2 female) then received extinction sessions and ended the experiment. The remaining female rat was mistakenly given shock at the start of the drug-free training session (rather than after 10 m), and was thus dropped from imaging analysis of the drug-free shock condition, but after extinction, this rat subsequently received scopolamine shock training and was thus included in analysis for that condition (see below). 4 rats (2 male, 2 female) were given their drug-free shock sessions after previously receiving barrier training as their first manipulation (so these rats were still naive to shock during drug-free shock avoidance training). 3 rats (1 male, 2 female) were given their drug-free shock session after previously receiving a scopolamine shock session (followed by extinction) as their first manipulation, and 2 rats (1 male, 1 female) were given their drug-free shock session after previously receiving both barrier training and a scopolamine shock session (followed by extinction). Among rats that were given scopolamine

shock sessions, 5 (2 males, 3 females) had not previously experienced shock at the time of their scopolamine shock avoidance training session, whereas 5 rats (3 males, 2 females) had previously received drug-free shock avoidance training followed by extinction. To compare imaging results across training conditions, rats from the drug-free condition were only included if they ran <60% as many trials during their first post-extinction session as during their final pre-training session (indicating that they had successfully acquired short path avoidance), whereas rats from the scopolamine shock condition were only included if they ran >60% as many trials during during their first post-extinction session as during their final pre-training session (indicating that scopolamine had successfully blocked avoidance learning).

Surgical procedures

Subjects were given two survival surgeries prior to behavior training in order to record fluorescent calcium activity from hippocampal CA1 cells. During the first surgery, rats were anesthetized with 5% isoflurane at 2.5 L/min of oxygen, then maintained at 2-2.5% isoflurane while a craniotomy was made above the dorsal hippocampus. Next, 1.2 uL of AAV9-Syn-GCamp7s (AddGene) was injected at .12uL/min just below the dorsal CA1 pyramidal layer (-3.6 AP, 2.5 ML, 2.6 DV) via a 10uL Nanofil syringe (World Precision Instruments) mounted in a Quintessential Stereotaxic Injector (Stoelting) controlled by a Motorized Lab Standard Stereotax (Harvard Apparatus). Left or right hemisphere was balanced across all animals. One week later, the rat was again induced under anesthesia and 4 skull screws were implanted to provide stable hold for the subsequent implant. The viral craniotomy was reopened to a diameter of 1.8 mm, and cortical tissue and corpus callosal fibers above the hippocampus were aspirated away using a 27 and 30 gauge blunt needle. Following this aspiration, and assuring no bleeding persisted in the craniotomy, a 1.8mm diameter Gradient Refractive INdex lens (“GRIN lens”, Edmund Optics) was implanted over the hippocampus and cemented in

place with methacrylate bone cement (Simplex-P, Stryker Orthopaedics). The dorsal surface of the skull and the bone screws were cemented with the GRIN lens to ensure stability of the implant, while the dorsal surface of the implanted lens was left exposed.

Two to three weeks later, rats were again placed under anesthesia in order to cement a 3D printed baseplate above the lens. First a second GRIN lens was optically glued (Norland Optical Adhesive 68, Edmund Optics) to the surface of the implanted lens and cured with UV light. The pitch of each GRIN lens is .25, so implanting 2 together provides a .5 pitch. This half pitch provides translation of the image at the bottom surface of the lenses to the top while maintaining the focal point below the lens. This relay implant enables access to tissue deep below the skull surface. Magnification of the image is performed by the miniscope. The miniscope was placed securely in the baseplate and then mounted to the stereotax to visualize the calcium fluorescence and tissue. The baseplate was then cemented in place above the relay lenses at the proper focal plane and allowed to cure. Once rats had been baseplated, they were placed on food restriction to reach a goal weight of 85% *ad lib* weight and then began behavioral training. Time between the beginning of the surgical procedures and the start of behavior training was typically 6-8 weeks.

Histology

At the end of the experiment, rats were anesthetized with isoflurane, intraperitoneally injected with 1 mL of pentobarbital, then transcardially perfused with 100 mL of 0.01M PBS followed by 200 mL of 4% paraformaldehyde in 0.01M PBS to fix the brain tissue. Brains were sectioned at 40 μm thickness on a cryostat (Leica), mounted on gelatin prepared slides, then imaged on a confocal microscope (Zeiss) to confirm GFP expression and GRIN lens placement (see example in Fig. 2A).

MiniLFOV calcium imaging system

To record calcium activity during unrestrained behavior, we utilized a large field of view version of the Miniscope imaging system, “MiniLFOV” (Guo et al., 2021). This open-source epifluorescence imaging camera weighs 13.9 g with a 3.6 x 2.3 mm field of view while maintaining a 2.5 um resolution at the center of view and 4.4 um at the periphery. The MiniLFOV can record at 22 Hz, has a 5MP CMOS imaging sensor, an electrowetting lens for digitally setting the focal plane, and a modular lens configuration to enable a longer working distance (either 1.8 mm, used here, or 3.5 mm). The system is 20x more sensitive than previous v3 Miniscopes, and twice as sensitive as current v4 Miniscopes. Power, communication, and image data are packed into a flexible 50 Ω coaxial cable (CW2040-3650SR, Cooner Wire) using power-over-coax filtering and a serializer/deserializer pair for bi-directional control communication with I^2C protocol and uni-directional high bandwidth data streaming. The MiniLFOV device interfaces with UCLA open-source Miniscope DAQ Software to stream, visualize and record neural dynamics and head orientation data. This DAQ platform and software allow for excitation intensity adjustment, focus change, image sensor gain selection, and frame rate setting. See the MiniLFOV website (github.com/Aharoni-Lab/Miniscope-LFOV) and methods paper (Guo et al., 2021) for further details and printable part files.

Behavior tracking

A webcam mounted in the behavior room tracked a red LED located on the top of the miniscope and this video was saved alongside the calcium imaging via the miniscope software with synchronized frame timestamps. These behavior video files were initially processed by custom python code, where all the session videos were concatenated together into one tiff stack, downsampled to 15 frames per second, the median of the stack was subtracted from each image, and finally they were all rescaled to the original 8-bit range to yield the same maximum and minimum values before subtraction. Background subtracted behavior videos

were then processed in MATLAB. The rat's position in each frame was determined using the location of the red LED on the camera. Extracted positions were then rescaled to remove the camera distortion and convert the pixel position to centimeters according to the maze size. Positional information was then interpolated to the timestamps of the calcium imaging video.

Behavioral performance measures and criteria

During the initial phase of training where rats learn to prefer the short path over the long path on the maze, rats were required to reach a criterion of earning at least 2 rewards per minute by taking the short path and earning at least twice as many rewards on the short versus long path during a single 15 min session. After reaching this criterion, rats were given avoidance training in the next session as explained in Results. After a single avoidance training session, rats received standard (non-shock) sessions until avoidance behavior was extinguished. Rats were considered to have extinguished avoidance behavior on the first post-training day that they recovered to the original criterion (defined above) for preferring the short path.

48 h retention of short path avoidance was quantified by the ratio $A = N_{+48}/N_{-48}$, where N_{+48} and N_{-48} are the number of rewards earned on the short path during the first session after and before the training session, respectively. Hence, lower values of A indicated better 48 h retention of short path avoidance. In the drug-free shock condition, an individual rat was considered to show failed 48 h retention of short path avoidance if A>0.6, which was the cutoff for the top quartile of A values in all rats (n=11) from which imaging as successfully obtained during the drug-free shock condition (of the 14 rats that received drug-free shock training, one was omitted from imaging analysis because shocks were mistakenly delivered at the start of the session, and two were omitted because they failed to ever reach criterion for extinction of avoidance behavior after multiple post-training sessions). In the scopolamine shock condition,

an individual rat was considered to show successful 48 h retention of short path avoidance if A <0.31, which was the cutoff for the bottom quartile of A values in all rats (n=9) from which imaging was successfully obtained during the scopolamine shock condition (of the 10 rats that received scopolamine shocks, one was omitted from imaging analysis because the the GRIN lens shifted and imaging was lost prior to the avoidance training session).

Behavioral downsampling

Since behavior on the maze was altered by training and drug administration (Fig. 1), imaging analyses only included data from beeline trials during which rats ran from one end of the track to the other with no change in direction. This assured that rats were behaving as similarly as possibly during data collection in all sessions. Beeline trials from each session were then further downsampled prior to imaging analyses, to control for potential effects of behavior or sampling differences on the outcome of imaging analyses.

For comparisons of pre-training versus training sessions (Fig. 2C-H) in the drug-free versus scopolamine shock conditions, it was necessary to correct for two imbalances in behavior between the drug-free versus scopolamine conditions (Supplementary Fig. 2A): 1) rats ran more slowly (and thus also ran fewer beeline trials) during training sessions on scopolamine than drug-free, and 2) rats ran more pre-training trials per session in the scopolamine than the drug free condition. To correct for imbalance #1, we computed that the mean number of beeline trials (in the LR and RL directions combined) during training in the scopolamine condition (23.85 trials) was 64% of mean beeline trials in the drug-free condition (37.22 trials); since running speed was also slower for scopolamine training, we sorted each rat's drug free training beeline trials in order of running speed, and omitted the fastest 36% of trials from each running direction (rounded to the nearest integer). This simultaneously equalized beeline trial counts and running

speeds during training sessions between the drug-free versus scopolamine conditions. To correct for imbalance #2, we computed that the mean number of beeline trials during pre-training (in the LR and RL directions combined) in the drug-free condition (53.78 trials) was 71% of mean beeline trials in the drug-free condition (76.0 trials);we thus omitted the last 29% of trials from each running direction in the pre-training session. This equalized trials counts across training conditions without significantly affecting mean running speeds. Also, since omitted pre-training trials were removed from the end of the session, the effective duration of pre-training sessions was reduced from 15 min down to a shorter duration that was more similar to the 10 min pre-shock period during which beeline trials were sampled from the training session. After these behavioral downsampling measures had been taken, rats in both conditions still ran fewer beeline trials during the analyzed portion of the training session (the first 10 min prior to shock delivery) than during the included portion of the pre-training session, as a consequence of the fact that scopolamine rats ran fewer trials in the training session and this low trial count had to be matched in the drug-free group. But the difference in trial counts between pre-training and training sessions, though large, was similar for the drug-free and scopolamine training conditions, and was therefore assumed not to be a confound in analyses of the training condition effects (Figs. 2C-H).

For comparisons of pre-training versus post-extinction sessions (Fig. 3), it was necessary to correct for two imbalances in behavior between the drug-free versus scopolamine conditions (Supplementary Fig. 2A): 1) rats in the drug-free shock condition tended to run fewer laps at lower speeds during the post than pre session (presumably because they still had some residual fear of the short path even after reaching the extinction criterion) whereas rats in the barrier condition tended to run more laps at higher speeds during the post than the pre session (presumably because they continued to acquire a preference for the short path without being interrupted by avoidance learning), and 2) during both the pre and post sessions, rats in the

scopolamine shock condition ran more short path beeline trials than rats in the other two conditions. Imbalance #1 was correct in two steps. The first step was to take a difference between the number of pre and post session trials for each rat in the drug free condition: $N_{diff}^{DF} = N_{pre}^{DF} - N_{post}^{DF}$. Trials from the pre session were then sorted by speed, and the fastest N_{diff}^{DF} trials were removed from the pre session, which equalized the number of pre and post session beeline trials while also making their mean running speeds much more similar, so that there was no longer a significant running speed difference (Fig. 3B, right). The second step was to take a difference between the number of pre and post session trials for each rat in the barrier condition: $N_{diff}^{BAR} = N_{post}^{BAR} - N_{pre}^{BAR}$. Trials from the post session were then sorted by speed, and the fastest N_{diff}^{BAR} trials were removed from the post session, which equalized the number of pre and post session beeline trials while also making their mean running speeds much more similar, so that there was no longer a significant running speed difference (Fig. 3B, right). Then an additional 20% of the fastest trials were removed from both sessions to render the mean number of beeline trials per session similar across the drug-free and barrier conditions. To correct for imbalance #2, the absolute difference was taken between the number of pre and post session trials for each rat in the drug free condition: $N_{diff}^{SCOP} = \left|N_{pre}^{SCOP} - N_{post}^{SCOP}\right|$; trials from the scopolamine shock condition were then sorted by running speed, and the number of pre and post trials was equalized by removing fastest N_{diff}^{SCOP} trials from whichever session had fewer trials in a given rat. Then an additional 25% of the fastest trials were removed from both sessions to render the mean number of beeline trials per session similar across the drug-free and scopolamine shock conditions.

Spatial tuning properties

To analyze acute effects of scopolamine on spatial tuning properties, we measured each peak Af/s rate, out-of-field Af/s rate, tuning width, and spatial information content from place cell tuning curves. Peak Af/s rate was defined as the maximum Af/s rate observed for any of the 23 bins in the tuning curve. Out-of-field Af/s rate was defined as the mean rate in the subset of spatial bins that had rates <50% of the peak Af/s rate. Tuning width was computed as $W \times N_{50}$, where W=10.8 cm is the width if each bin and N_{50} is the number of bins that had rates >50% of the peak Af/s rate. Spatial information content was measured in units of bits per active frame (bits/Af), which was computed as (Skaggs et al., 1993):

$$-\overline{r_B} log_2(\overline{r_B}) + \sum_{i=1}^{B} r_i p_i log_2(r_i)$$

where B is the set of spatial bins with non-zero mean Af/s rates, r_i is the mean Af/s rate in spatial bin *i*, p_i is the probability that the rat was occupying bin *i*, and $\overline{r_B}$ is the mean Af/s rate over all bins in the set B.

Selection of place cells

Stable place cells were identified in each imaging session by randomly splitting the session's beeline trials (separately for each running direction) into two halves, and then computing two spatial tuning curves, one for each randomly chosen half of the beeline trials. A Pearson correlation coefficient (*R*) between these two tuning curves was then computed, and its p-value was recorded. A cell was classified as a place cell in a given session if the median p-value for *R* was <.01 over 200 iterations of random beeline splits in either of the two running directions. To be classified as a place cell, a neuron also had to generate an average of at least one inferred spike per beeline trial, and was not permitted to fire at >70% of its peak inferred

spike rate over more than 50% of the track (this was done to exclude likely interneurons, and thereby restrict analysis to putative pyramidal neurons).

Recurring place fields

A recurring place field was defined as an LR or RL tuning curve that: 1) met the spatial selectivity criteria described above during at least one of the two sessions, and 2) contained active frames (that is, generated at least one inferred spike) during subsampled beeline trials in the specified running direction from both sessions. Place cell tuning curves were excluded from the between-session heatmap pair if they contained *non-recurring place fields*, defined as those that: 1) met spatial selectivity criteria in during one of the two sessions, but 2) generated no inferred spikes (and thus went completely undetected) during subsampled beeline trials in the specified running direction from the other session.

Shock responses

To analyze shock-evoked responses of CA1 place cells, we identified each frame during which the rat made an entry into the electrified shock zone, and noted in which direction the rat was running when shock onset began. For each entry into the shock zone, a significant shock-evoked response occurred when the count of active frames in a 2 s window after entry into the electrified shock zone exceeded the confidence limit ($p<.01$) for a Poisson fit to the baseline distribution of active frame counts from prior visits (during the first 10 m of the session) to unelectrified shock zone in the same running direction. Most rats experienced the shock in both running directions before they began to avoid the short path, but a few rats only experienced the shock in one direction, and in a small number of rats, more than two shocks

were received before the rat began avoiding the short path. To equalize statistical power for detecting shock responses across all rats (regardless of the shocks they received), a neuron was classified as shock responsive only if it exhibited a significant shock response during the rat's first or second visit (or both) to the electrified shock zone; later visits to the shock zone were not considered, so that place cells would not have a higher likelihood of being classified as shock responsive in rats that made more visits to the shock zone.

To compute population averaged responses of place cells to shocks, only the first significant shock-evoked response of each shock responsive place cell (from either the first or second shock encounter, whichever yielded the first significant response) was included in the average, so that each cell's contribution to the average always came from a single significant shock response trial, and therefore did not vary depending upon the number of shocks different animals received. For shock responsive place cells, the population average included only the first shock encounter (which by definition failed to elicit a significant shock response), so that again, each cell's contribution to the average came from a single trial.

Distributions of tuning curve peak locations (Fig, 7A, right) for shock responsive place cells included only tuning curve peaks for the running direction in which the rat received its first significant shock-evoked response (from either the first or second shock encounter, whichever yielded the first significant response). Distributions of tuning curve peak locations for shock shock responsive place cells included tuning curve peaks from both running directions if the rat received its first and second shock in different directions, but if the first and second shock were both received in the same running direction, then only the tuning curve peak for that direction was included in the distribution of peak locations.

To assess whether a place cell's tuning curve peak was on the approaching versus departing side of the shock zone, the 23-bins of the tuning curve were reflected across the middle (bin 13) for RL tuning curves, but not for LR tuning curves, so that for both running directions, tuning curve peaks in bins 1-12 were on the approaching side of the shock zone, and

peaks in bins 14-23 were on the departing side of the shock zone. For tuning curves with peaks in the center (bin 13), an additional step was taken to measure the percentage of the area under the tuning curve on either side of center. If the area in bins 1-12 was greater than in bins 14-23, then the tuning curve peak was considered to be on the approaching side, otherwise, it was considered to be on the departing side.

Position decoding

For decoding analysis, frame positions in one imaging session were predicted using place cell heatmaps derived from a different session. For each analyzed pair of pre- and post-sessions, decoding was performed using memoryless Bayesian inference (Davidson et al., 2009; Zhang et al., 1998) with place maps constructed from each running direction. Post-training positions were predicted from pre-training heatmaps (pre→post), and vice versa (post→pre), taking the maximally likely position bin at each frame, and results from both directions were averaged together to obtain the results in Fig. 3G. A subsampling procedure was used to equalize the number of place cells used for each running direction (LR and RL, 100 subsample iterations), so that any observed differences in decoding performance were not attributable differences in the sizes of the population vectors (that is, the number of recurring place cells) that were used for pre-training versus cross-training decoding.

The *decoding error* (DE) in each frame was computed as the absolute error (in cm) between the rat's actual versus predicted position in that frame, $DE=abs(x_{act}-x_{pred})$. The *shuffled decoding error* ($DE_{shuffle}$) was derived in the same manner, except that place cells in the population vector were randomly permuted against their place maps before deriving the predicted position, x_{pred}. Shuffled decoding error was computed multiple times per frame using different random place cell permutations (n=2000 shuffles). The decoding error in a given position bin was measured as the median of the absolute difference (in cm) between the rat's

actual versus predicted position over all visits to that bin. The non-shuffled decoding error was subtracted from the median $DE_{shuffle}$ to obtain the *accuracy gain* in each frame, G=median($DE_{shuffle}$)-DE, which measured by how many cm the decoding error was reduced when position was predicted from non-shuffled rather than shuffled population vectors. The median value of G was derived for all frames in each actual position bin, x, yielding an accuracy gain measurement at each position on the track, $G(x)$=median(G_{x1}, G_{x2}, … G_{xn}). Accuracy gain was computed separately at each position in each running direction (LR and RL) and each decoding direction (pre→post and post→pre) to obtain four different G(x) values per session pair: $G^{LR}_{pre\rightarrow post}(x)$, $G^{RL}_{pre\rightarrow post}(x)$, $G^{LR}_{post\rightarrow pre}(x)$, and $G^{RL}_{post\rightarrow pre}(x)$. For statistical analyses, each of these four values was treated as an independent observation at each position. Accuracy gains tended to be greater near the ends of the track than in the middle, but this was mainly a consequence of bias in the G(x) accuracy measure, rather than better decoding at the ends of the track, because greater reductions of G(x) were attainable near the ends of the track, where x_{act}-x_{pred} could span the entire track length, than in the middle, where x_{act}-x_{pred} could only span half the track length at most. To eliminate this positional bias, we used Wilcoxon signed-rank tests (rather than subtraction) to test whether the median error difference, $DE_{shuffle}$-DE, differed significantly from zero (see Methods). P-values from the Wilcoxon tests provided a measure of decoding performance that was unbiased by track position, but these P-values were non-normally distributed, and thus could not be analyzed to test for interaction effects using parametric statistics. We therefore took the negative log of the Wilcoxon P value and multiplied by the sign of G to derive a *decoding accuracy index*, DAI = $-\log_{10}$ (P) x sign(G) - 2, which was both normally distributed and unbiased by track position. Subtracting 2 at the end of the expression was done so that DAI = 0 would correspond to p=.01 for more significant decoding from unshuffled than shuffled population vectors, since $\log_{10}$ .01=2.

REFERENCES

Alvernhe A, Save E, Poucet B. 2011. Local remapping of place cell firing in the Tolman detour task. Eur J Neurosci 33:1696–1705. doi:10.1111/j.1460-9568.2011.07653.x

Anagnostaras SG, Maren S, Fanselow MS. 1995. Scopolamine Selectively Disrupts the Acquisition of Contextual Fear Conditioning in Rats. Neurobiol Learn Mem 64:191–194. doi:10.1006/nlme.1995.0001

Anagnostaras SG, Maren S, Sage JR, Goodrich S, Fanselow MS. 1999. Scopolamine and Pavlovian Fear Conditioning in Rats: Dose-Effect Analysis. Neuropsychopharmacol 21:731–744. doi:10.1016/s0893-133x(99)00083-4

Atri A, Sherman S, Norman KA, Kirchhoff BA, Nicolas MM, Greicius MD, Cramer SC, Breiter HC, Hasselmo ME, Stern CE. 2004. Blockade of Central Cholinergic Receptors Impairs New Learning and Increases Proactive Interference in a Word Paired-Associate Memory Task. Behav Neurosci 118:223–236. doi:10.1037/0735-7044.118.1.223

Barnes CA. 1979. Memory deficits associated with senescence: A neurophysiological and behavioral study in the rat. J Comp Physiol Psych 93:74–104. doi:10.1037/h0077579

Barnes CA, Nadel L, Honig WK. 1980. Spatial memory deficit in senescent rats. Can J Psychology Revue Can De Psychologie 34:29–39. doi:10.1037/h0081022

Barnes CA, Suster MS, Shen J, McNaughton BL. 1997. Multistability of cognitive maps in the hippocampus of old rats. Nature 388:272–275. doi:10.1038/40859

Barten DM, Albright CF. 2008. Therapeutic Strategies for Alzheimer's Disease. Mol Neurobiol 37:171–186. doi:10.1007/s12035-008-8031-2

Bittner KC, Grienberger C, Vaidya SP, Milstein AD, Macklin JJ, Suh J, Tonegawa S, Magee JC. 2015. Conjunctive input processing drives feature selectivity in hippocampal CA1 neurons. Nat Neurosci 18:1133–1142. doi:10.1038/nn.4062

Blair HT, Schafe GE, Bauer EP, Rodrigues SM, LeDoux JE. 2001. Synaptic Plasticity in the Lateral Amygdala: A Cellular Hypothesis of Fear Conditioning. Learn Memory 8:229–242. doi:10.1101/lm.30901

Bostock E, Muller RU, Kubie JL. 1991. Experience-dependent modifications of hippocampal place cell firing. Hippocampus 1:193–205. doi:10.1002/hipo.450010207

Brazhnik E, Borgnis R, Muller RU, Fox SE. 2004. The Effects on Place Cells of Local Scopolamine Dialysis Are Mimicked by a Mixture of Two Specific Muscarinic Antagonists. J Neurosci 24:9313–9323. doi:10.1523/jneurosci.1618-04.2004

Cai DJ, Aharoni D, Shuman T, Shobe J, Biane J, Song W, Wei B, Veshkini M, La-Vu M, Lou J, Flores SE, Kim I, Sano Y, Zhou M, Baumgaertel K, Lavi A, Kamata M, Tuszynski M, Mayford M, Golshani P, Silva AJ. 2016. A shared neural ensemble links distinct contextual memories encoded close in time. Nature 534:115–118. doi:10.1038/nature17955

Colgin LL, Moser EI, Moser M-B. 2008. Understanding memory through hippocampal remapping. Trends Neurosci 31:469–477. doi:10.1016/j.tins.2008.06.008

d'Aquin S, Szonyi A, Mahn M, Krabbe S, Gründemann J, Lüthi A. 2022. Compartmentalized dendritic plasticity during associative learning. Science 376:eabf7052. doi:10.1126/science.abf7052

Dannenberg H, Young K, Hasselmo M. 2017. Modulation of Hippocampal Circuits by Muscarinic and Nicotinic Receptors. Front Neural Circuit 11:102. doi:10.3389/fncir.2017.00102

Davidson TJ, Kloosterman F, Wilson MA. 2009. Hippocampal Replay of Extended Experience. Neuron 63:497–507. doi:10.1016/j.neuron.2009.07.027

Decker MW, Tran T, McGaugh JL. 1990. A comparison of the effects of scopolamine and diazepam on acquisition and retention of inhibitory avoidance in mice. Psychopharmacology 100:515–521. doi:10.1007/bf02244005

Digby GJ, Shirey JK, Conn PJ. 2010. Allosteric activators of muscarinic receptors as novel approaches for treatment of CNS disorders. Mol Biosyst 6:1345–1354. doi:10.1039/c002938f

Douchamps V, Jeewajee A, Blundell P, Burgess N, Lever C. 2013. Evidence for Encoding versus Retrieval Scheduling in the Hippocampus by Theta Phase and Acetylcholine. J Neurosci 33:8689–8704. doi:10.1523/jneurosci.4483-12.2013

Dragoi G, Harris KD, Buzsáki G. 2003. Place Representation within Hippocampal Networks Is Modified by Long-Term Potentiation. Neuron 39:843–853. doi:10.1016/s0896-6273(03)00465-3

Frick KM, Stillner ET, Berger-Sweeney J. 2000. Mice are not little rats: species differences in a one-day water maze task. Neuroreport 11:3461–3465. doi:10.1097/00001756-200011090-00013

Frotscher M, Misgeld U. 1989. Central Cholinergic Synaptic Transmission, Experientia Supplementum. doi:10.1007/978-3-0348-9138-7

Geiller T, Sadeh S, Rolotti SV, Blockus H, Vancura B, Negrean A, Murray AJ, Rózsa B, Polleux F, Clopath C, Losonczy A. 2022. Local circuit amplification of spatial selectivity in the hippocampus. Nature 601:105–109. doi:10.1038/s41586-021-04169-9

Green A, Ellis KA, Ellis J, Bartholomeusz CF, Ilic S, Croft RJ, Phan KL, Nathan PJ. 2005. Muscarinic and nicotinic receptor modulation of object and spatial n-back working memory in humans. Pharmacol Biochem Be 81:575–584. doi:10.1016/j.pbb.2005.04.010

Grewe BF, Gründemann J, Kitch LJ, Lecoq JA, Parker JG, Marshall JD, Larkin MC, Jercog PE, Grenier F, Li JZ, Lüthi A, Schnitzer MJ. 2017. Neural ensemble dynamics underlying a long-term associative memory. Nature 543:670–675. doi:10.1038/nature21682

Guo C, Blair GJ, Sehgal M, Jimka FNS, Bellafard A, Silva AJ, Golshani P, Basso MA, Blair HT, Aharoni D. 2021. Miniscope-LFOV: A large field of view, single cell resolution, miniature microscope for wired and wire-free imaging of neural dynamics in freely behaving animals. Biorxiv 2021.11.21.469394. doi:10.1101/2021.11.21.469394

Hasselmo ME. 2006. The role of acetylcholine in learning and memory. Curr Opin Neurobiol 16:710–715. doi:10.1016/j.conb.2006.09.002

Hasselmo ME, McGaughy J. 2004. High acetylcholine levels set circuit dynamics for attention and encoding and low acetylcholine

levels set dynamics for consolidation. Prog Brain Res 145:207–231. doi:10.1016/s0079-6123(03)45015-2

Huang Z-B, Wang H, Rao X-R, Zhong G-F, Hu W-H, Sheng G-Q. 2011. Different effects of scopolamine on the retrieval of spatial memory and fear memory. Behav Brain Res 221:604–609. doi:10.1016/j.bbr.2010.05.032

Hunt DL, Linaro D, Si B, Romani S, Spruston N. 2018. A novel pyramidal cell type promotes sharp-wave synchronization in the hippocampus. Nat Neurosci 21:985–995. doi:10.1038/s41593-018-0172-7

Jarzebowski P, Tang CS, Paulsen O, Hay YA. 2021. Impaired spatial learning and suppression of sharp wave ripples by cholinergic activation at the goal location. Elife 10:e65998. doi:10.7554/elife.65998

Jiang L, Kundu S, Lederman JD, López-Hernández GY, Ballinger EC, Wang S, Talmage DA, Role LW. 2016. Cholinergic Signaling Controls Conditioned Fear Behaviors and Enhances Plasticity of Cortical-Amygdala Circuits. Neuron 90:1057–1070. doi:10.1016/j.neuron.2016.04.028

Josselyn SA, Tonegawa S. 2020. Memory engrams: Recalling the past and imagining the future. Science 367:eaaw4325. doi:10.1126/science.aaw4325

Keinath AT, Mosser C-A, Brandon MP. 2022. The representation of context in mouse hippocampus is preserved despite neural drift. Nat Commun 13:2415. doi:10.1038/s41467-022-30198-7

Kim EJ, Park M, Kong M-S, Park SG, Cho J, Kim JJ. 2015. Alterations of Hippocampal Place Cells in Foraging Rats Facing a “Predatory” Threat. Curr Biol 25:1362–1367. doi:10.1016/j.cub.2015.03.048

Kinsky NR, Sullivan DW, Mau W, Hasselmo ME, Eichenbaum HB. 2018. Hippocampal Place Fields Maintain a Coherent and Flexible Map across Long Timescales. Curr Biol 28:3578-3588.e6. doi:10.1016/j.cub.2018.09.037

Leutgeb JK, Leutgeb S, Treves A, Meyer R, Barnes CA, McNaughton BL, Moser M-B, Moser EI. 2005. Progressive Transformation of Hippocampal Neuronal Representations in “Morphed” Environments. Neuron 48:345–358. doi:10.1016/j.neuron.2005.09.007

Leutgeb S, Leutgeb JK, Barnes CA, Moser EI, McNaughton BL, Moser M-B. 2005. Independent Codes for Spatial and Episodic Memory in Hippocampal Neuronal Ensembles. Science 309:619–623. doi:10.1126/science.1114037

Lever C, Wills T, Cacucci F, Burgess N, O’Keefe J. 2002. Long-term plasticity in hippocampal place-cell representation of environmental geometry. Nature 416:90–94. doi:10.1038/416090a

Lombardo S, Maskos U. 2015. Role of the nicotinic acetylcholine receptor in Alzheimer’s disease pathology and treatment. Neuropharmacology 96:255–262. doi:10.1016/j.neuropharm.2014.11.018

Ma X, Zhang Y, Wang L, Li N, Barkai E, Zhang X, Lin L, Xu J. 2020. The Firing of Theta State-Related Septal Cholinergic Neurons Disrupt Hippocampal Ripple Oscillations via Muscarinic Receptors. J Neurosci 40:3591–3603. doi:10.1523/jneurosci.1568-19.2020

Mamad O, Agayby B, Stumpp L, Reilly RB, Tsanov M. 2019. Extrafield Activity Shifts the Place Field Center of Mass to Encode Aversive Experience. Eneuro 6:ENEURO.0423-17.2019. doi:10.1523/eneuro.0423-17.2019

Mankin EA, Sparks FT, Slayyeh B, Sutherland RJ, Leutgeb S, Leutgeb JK. 2012. Neuronal code for extended time in the hippocampus. Proc National Acad Sci 109:19462–19467. doi:10.1073/pnas.1214107109

Martin SJ, Grimwood PD, Morris RGM. 2000. Synaptic Plasticity and Memory: An Evaluation of the Hypothesis. Neurosci 23:649–711. doi:10.1146/annurev.neuro.23.1.649

Mau W, Hasselmo ME, Cai DJ. 2020. The brain in motion: How ensemble fluidity drives memory-updating and flexibility. Elife 9:e63550. doi:10.7554/elife.63550

McKenzie S, Huszár R, English DF, Kim K, Christensen F, Yoon E, Buzsáki G. 2021. Preexisting hippocampal network dynamics constrain optogenetically induced place fields. Neuron 109:1040-1054.e7. doi:10.1016/j.neuron.2021.01.011

Miller KJ, Botvinick MM, Brody CD. 2017. Dorsal hippocampus contributes to model-based planning. Nat Neurosci 20:1269–1276. doi:10.1038/nn.4613

Moita MAP, Rosis S, Zhou Y, LeDoux JE, Blair HT. 2004. Putting Fear in Its Place: Remapping of Hippocampal Place Cells during Fear Conditioning. J Neurosci 24:7015–7023. doi:10.1523/jneurosci.5492-03.2004

Moita MAP, Rosis S, Zhou Y, LeDoux JE, Blair HT. 2003. Hippocampal Place Cells Acquire Location-Specific Responses to the Conditioned Stimulus during Auditory Fear Conditioning. Neuron 37:485–497. doi:10.1016/s0896-6273(03)00033-3

Newman EL, Venditto SJC, Climer JR, Petter EA, Gillet SN, Levy S. 2017. Precise spike timing dynamics of hippocampal place cell activity sensitive to cholinergic disruption. Hippocampus 27:1069–1082. doi:10.1002/hipo.22753

Okada S, Igata H, Sasaki T, Ikegaya Y. 2017. Spatial Representation of Hippocampal Place Cells in a T-Maze with an Aversive Stimulation. Front Neural Circuit 11:101. doi:10.3389/fncir.2017.00101

O’Keefe J, Dostrovsky J. 1971. The hippocampus as a spatial map. Preliminary evidence from unit activity in the freely-moving rat. Brain Res 34:171–175. doi:10.1016/0006-8993(71)90358-1

O’Keefe J, Nadel L. 1978. The Hippocampus as a Cognitive Map. Oxford University Press.

Oler JA, Markus EJ. 2000. Age‐related deficits in the ability to encode contextual change: A place cell analysis. Hippocampus 10:338–350. doi:10.1002/1098-1063(2000)10:3<338::aid-hipo14>3.0.co;2-y

Ragozzino ME, Artis S, Singh A, Twose TM, Beck JE, Messer WS. 2012. The Selective M1 Muscarinic Cholinergic Agonist CDD-0102A Enhances Working Memory and Cognitive Flexibility. J Pharmacol Exp Ther 340:588–594. doi:10.1124/jpet.111.187625

Sanders H, Wilson MA, Gershman SJ. 2020. Hippocampal remapping as hidden state inference. Elife 9:e51140. doi:10.7554/elife.51140

Schoenenberger P, O’Neill J, Csicsvari J. 2016. Activity-dependent plasticity of hippocampal place maps. Nat Commun 7:11824. doi:10.1038/ncomms11824

Schuette PJ, Reis FMCV, Maesta-Pereira S, Chakerian M, Torossian A, Blair G, Wang W, Blair HT, Fanselow MS, Kao JC, Adhikari A. 2020. Long-term characterization of hippocampal remapping during contextual fear acquisition and extinction. J Neurosci

40:8329–8342. doi:10.1523/jneurosci.1022-20.2020

Shuman T, Aharoni D, Cai DJ, Lee CR, Chavlis S, Page-Harley L, Vetere LM, Feng Y, Yang CY, Mollinedo-Gajate I, Chen L, Pennington ZT, Taxidis J, Flores SE, Cheng K, Javaherian M, Kaba CC, Rao N, La-Vu M, Pandi I, Shtrahman M, Bakhurin KI, Masmanidis SC, Khakh BS, Poirazi P, Silva AJ, Golshani P. 2020. Breakdown of spatial coding and interneuron synchronization in epileptic mice. Nat Neurosci 23:229–238. doi:10.1038/s41593-019-0559-0

Skaggs WE, McNaughton BL, Gothard KM, Markus EJ. 1993. An information-theoretic approach for deciphering the hippocampal code. NIPS.

Solari N, Hangya B. 2018. Cholinergic modulation of spatial learning, memory and navigation. Eur J Neurosci 48:2199–2230. doi:10.1111/ejn.14089

Stachenfeld KL, Botvinick MM, Gershman SJ. 2017. The hippocampus as a predictive map. Nat Neurosci 20:1643–1653. doi:10.1038/nn.4650

Stranahan AM. 2011. Similarities and Differences in Spatial Learning and Object Recognition Between Young Male C57Bl/6J Mice and Sprague-Dawley Rats. Behav Neurosci 125:791–795. doi:10.1037/a0025133

Sun D, Unnithan RR, French C. 2021. Scopolamine Impairs Spatial Information Recorded With “Miniscope” Calcium Imaging in Hippocampal Place Cells. Front Neurosci-switz 15:640350. doi:10.3389/fnins.2021.640350

Svoboda J, Popelikova A, Stuchlik A. 2017. Drugs Interfering with Muscarinic Acetylcholine Receptors and Their Effects on Place Navigation. Frontiers Psychiatry 8:215. doi:10.3389/fpsyt.2017.00215

Tanila H, Ku S, Kloosterman F, Wilson MA. 2018. Characteristics of CA1 place fields in a complex maze with multiple choice points. Hippocampus 28:81–96. doi:10.1002/hipo.22810

Vales K, Stuchlik A. 2005. Central muscarinic blockade interferes with retrieval and reacquisition of active allothetic place avoidance despite spatial pretraining. Behav Brain Res 161:238–244. doi:10.1016/j.bbr.2005.02.012

Vandecasteele M, Varga V, Berényi A, Papp E, Barthó P, Venance L, Freund TF, Buzsáki G. 2014. Optogenetic activation of septal cholinergic neurons suppresses sharp wave ripples and enhances theta oscillations in the hippocampus. Proc National Acad Sci 111:13535–13540. doi:10.1073/pnas.1411233111

Wallenstein GV, Vago DR. 2001. Intrahippocampal Scopolamine Impairs Both Acquisition and Consolidation of Contextual Fear Conditioning. Neurobiol Learn Mem 75:245–252. doi:10.1006/nlme.2001.4005

Wang ME, Wann EG, Yuan RK, Álvarez MMR, Stead SM, Muzzio IA. 2012. Long-Term Stabilization of Place Cell Remapping Produced by a Fearful Experience. J Neurosci 32:15802–15814. doi:10.1523/jneurosci.0480-12.2012

Wang ME, Yuan RK, Keinath AT, Álvarez MMR, Muzzio IA. 2015. Extinction of Learned Fear Induces Hippocampal Place Cell Remapping. J Neurosci 35:9122–9136. doi:10.1523/jneurosci.4477-14.2015

Wilson IA, Ikonen S, Gureviciene I, McMahan RW, Gallagher M, Eichenbaum H, Tanila H. 2004. Cognitive Aging and the Hippocampus: How Old Rats Represent New Environments. J Neurosci 24:3870–3878. doi:10.1523/jneurosci.5205-03.2004

Wilson IA, Ikonen S, McMahan RW, Gallagher M, Eichenbaum H, Tanila H. 2003. Place cell rigidity correlates with impaired spatial learning in aged rats. Neurobiol Aging 24:297–305. doi:10.1016/s0197-4580(02)00080-5

Wirtshafter HS, Disterhoft JF. 2022. In Vivo Multi-Day Calcium Imaging of CA1 Hippocampus in Freely Moving Rats Reveals a High Preponderance of Place Cells with Consistent Place Fields. J Neurosci JN-RM-1750-21. doi:10.1523/jneurosci.1750-21.2022

Zhang K, Ginzburg I, McNaughton BL, Sejnowski TJ. 1998. Interpreting Neuronal Population Activity by Reconstruction: Unified Framework With Application to Hippocampal Place Cells. J Neurophysiol 79:1017–1044. doi:10.1152/jn.1998.79.2.1017

Ziv Y, Burns LD, Cocker ED, Hamel EO, Ghosh KK, Kitch LJ, Gamal AE, Schnitzer MJ. 2013. Long-term dynamics of CA1 hippocampal place codes. Nat Neurosci 16:264–266. doi:10.1038/nn.3329

Zylla MM, Zhang X, Reichinnek S, Draguhn A, Both M. 2013. Cholinergic Plasticity of Oscillating Neuronal Assemblies in Mouse Hippocampal Slices. Plos One 8:e80718. doi:10.1371/journal.pone.0080718

SUPPLEMENTARY FIGURES

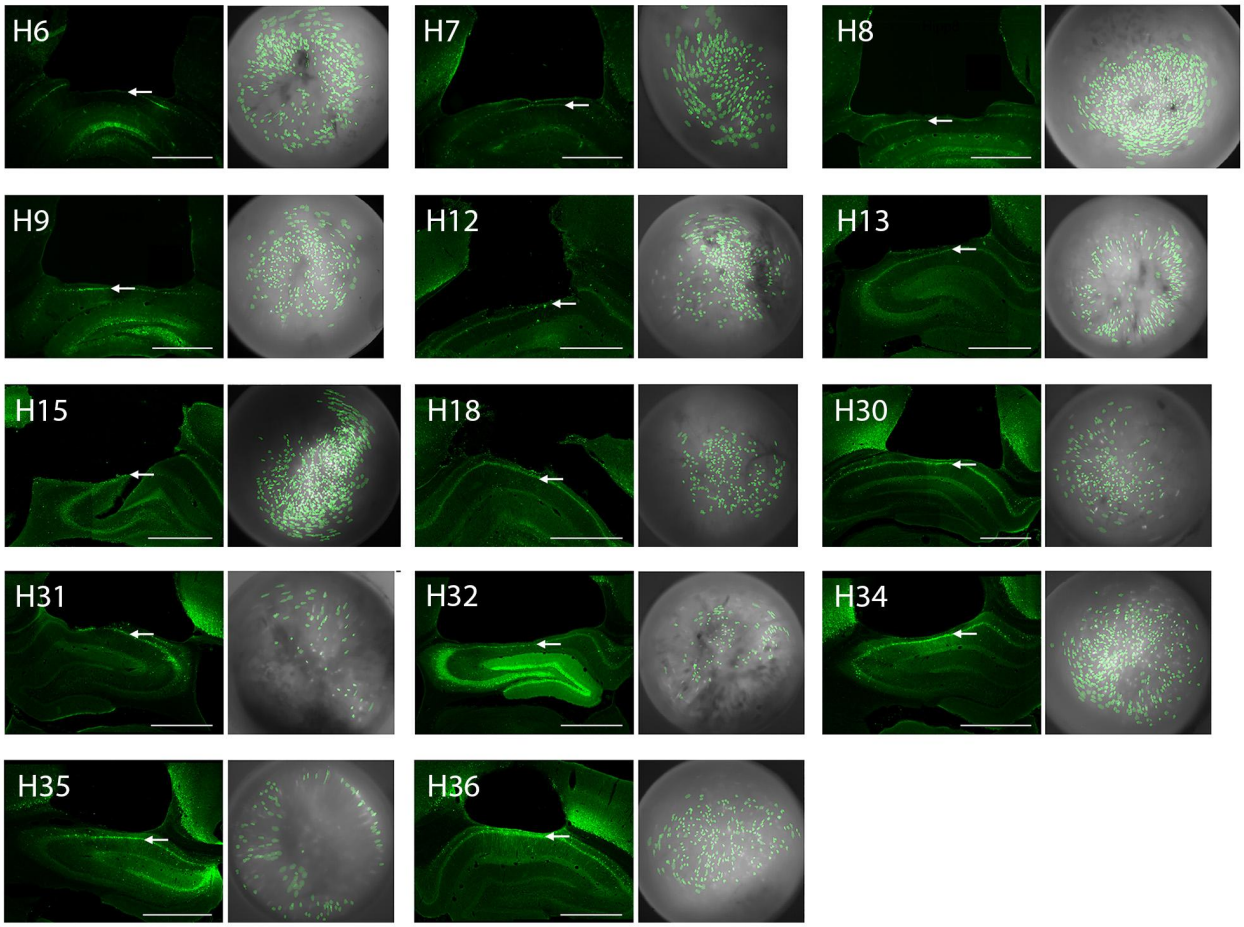

Supplementary Figure 1. *GRIN lens placements and cell contours for imaged neurons in CA1.* The left image in each pair shows a photomicrograph of the GRIN lens placement for one of the rats in the study; arrows point to the CA1 layer, scale bar = 1 mm. The right image in each pair shows cell contours (green) identified by CNMFe superimposed over cropped images of the MiniLFOV's view through the 1.8 mm GRIN lens; the image shown for each rat was obtained from the day of the rat's drug-free shock training session. Figure shows results from 14 rats that were included in imaging data analysis (one rat that was included in the behavior analysis but dropped from image analysis is not shown).

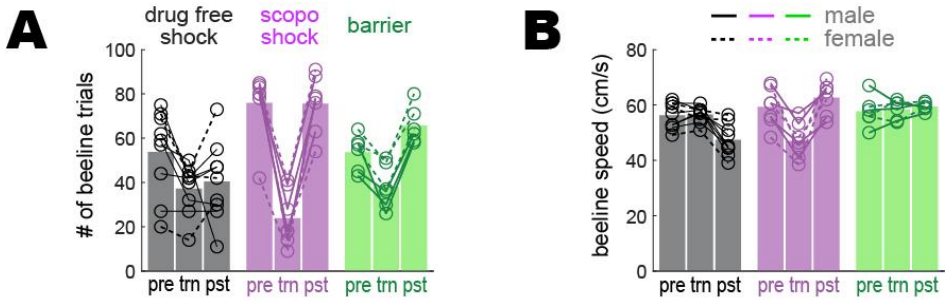

Supplementary Figure 2. *Beeline trial counts and running speeds prior to downsampling.* To control for any possible confounding effects of behavior upon imaging results, analyses presented in the main text were performed on behavioral data that was downsampled to equalize the number of beeline trials and median running speed across imaging sessions (see Methods). Graphs plotted here show the rats' behavior prior to downsampling beeline trials in the drug-free shock condition for rats that retained avoidance learning (n=9), scopolamine shock condition for rats that failed to retain avoidance learning (n=7), and barrier training condition (n=6). *A*) Number of beeline trials during pre-training (pre), training (trn), and post-extinction (pst) sessions prior to downsampling; a 3x3 mixed ANOVA yielded a marginal main effect of training condition (drug free shock, scopolamine shock, barrier: $F_{2,19}$=3.5, p=.0509), a significant main effect of session (pre, trn, pst: $F_{2,38}$=51.5, p=1.49e^{-11}), and a significant interaction ($F_{4,38}$=13.9, p=4.37e^{-7}). In all training conditions there were fewer trials during 'trn' sessions because data only came from the first 10 min (prior to shock or barrier introduction) of the training sessions, compared with 15 min of data for other session types. For the drug-free shock condition, the mean number of beeline trials is marginally lower during 'pst' than 'pre' sessions (paired t_8=2.1, p=.0676; uncorrected) because despite having reached the extinction criteria during the 'pst' session, rats persisted in showing some avoidance of the short path and thus earned fewer short path rewards during the 'pst' session. *B*) Median beeline running speed during per session prior to downsampling; a 3x3 mixed ANOVA yielded a marginal main effect of training condition (drug free shock, scopolamine shock, barrier: $F_{2,19}$=3.07, p=.0698), a significant main effect of session (pre, trn, pst: $F_{2,38}$=5.08, p=.0111), and a significant interaction ($F_{4,38}$=20.8, p=3.74e^{-9}). Uncorrected post-hoc paired t-tests found that for the drug-free shock condition, beeline running speed was significantly lower during 'pst' than 'pre' (t_8=4.4, p=.0022) or 'trn' (t_8=4.7, p=.0015) sessions; this was because despite having reached the avoidance extinction criteria during the 'pst' session, rats persisted in running more a bit slowly on the short path after avoidance extinction. In addition, during 'trn' sessions given on scopolamine, rats ran more slowly during 'trn' sessions than during 'pre' (t_6=5.5, p=.0015) or 'pst' (t_6=5.2, p=.0019) sessions (both of which were given drug free) because the drug acutely reduced running speeds on the maze, as reported in the main text.

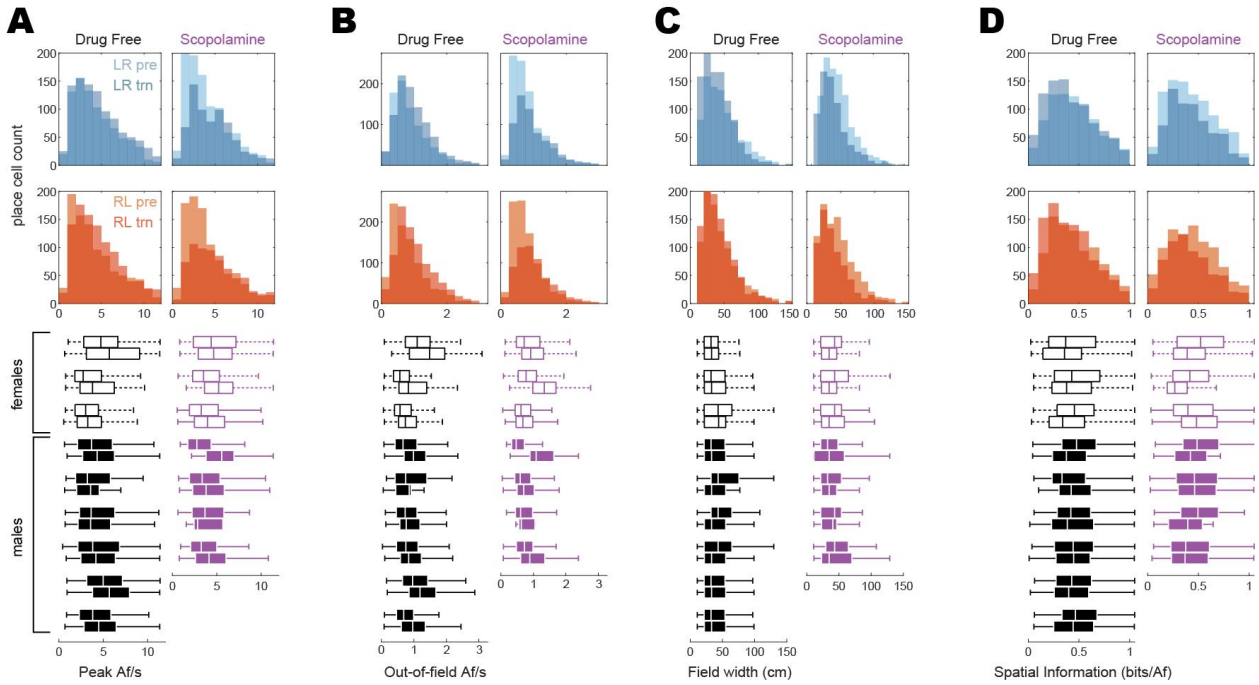

Supplementary Figure 3. *Distributions of place cell tuning properties.* Histograms at top compare pre-training and training session distributions of firing properties measured from tuning curves that were spatially tuned in the LR (top row, blue) or RL (second from top row, red) direction during one or both sessions. Boxplots below histograms show each rat's median and range of tuning property values for LR and RL tuning curves combined; boxplot medians for each rat are the same values plotted for each rat in Fig. 2F of the Results. *A*) *Peak Af/s rates*. From the histograms, it can be seen that scopolamine acutely reduces the proportion of tuning curves peaks that are <5 Af/s while having little effect on the frequency of peaks that are >5 Af/s. *B*) *Out-of-field Af/s rates*. Similar to peak Af/s rates, scopolamine acutely reduced the incidence of low out-of-field rates (<1 Af/s), while having little effect on the incidence of higher rates (>1 Af/s). *C*) *Field widths*. Scopolamine slightly narrows the width of place fields; since the field width is defined as the number of spatial bins that exceed 50% of the peak rate, this slight narrowing of place fields may be related to the fact that peak Af/s rates are higher on scopolamine (see 'A'). *D*) *Spatial information*. Distributions of bits/Af showed little change on scopolamine.

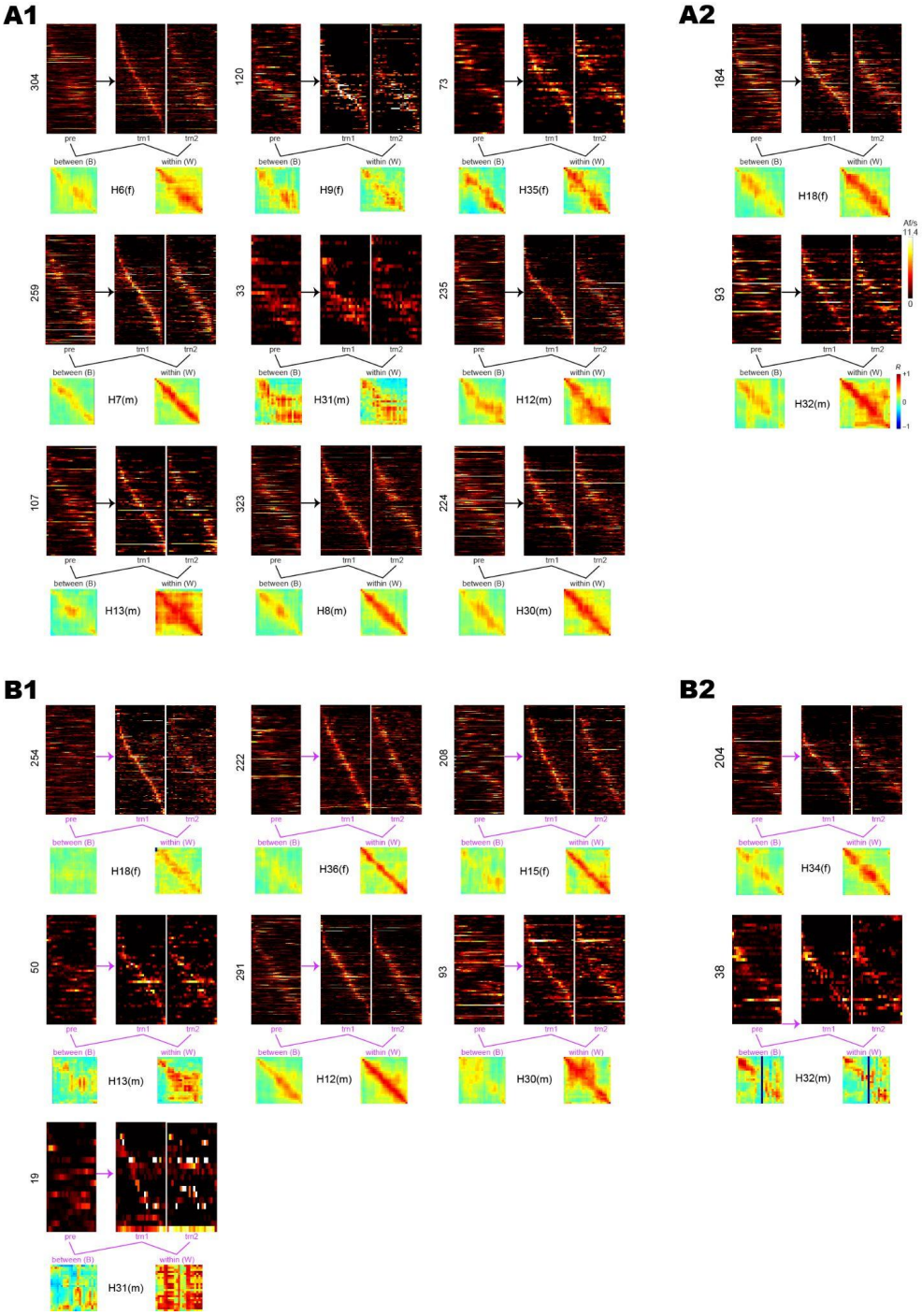

Supplementary Figure 4. *Pre-training and training session data from individual rats.* As in Fig. 2H, heatmaps are shown for the pre, trn1, and trn2 sessions, with between- (pre vs trn1) and within- (trn1 vs trn2) session correlation matrices below heatmaps. For brevity, LR and RL tuning curves are co-sorted within heatmaps so that cells meeting spatial selectivity criteria in both running directions contribute two rows to each heatmap (one per direction), whereas cells meeting selectivity criteria in only one direction contribute only row to each heatmap. *A1*) Rats (n=9) from the drug-free shock condition that showed 48 h avoidance retention. *A2*) Rats (n=2) from the drug-free shock condition that failed to show 48 h avoidance retention. *B1*) Rats (n=7) from the scopolamine condition that failed to show 48 h avoidance retention. *B2*) Rats (n=2) from the scopolamine shock condition that showed 48 h avoidance retention.

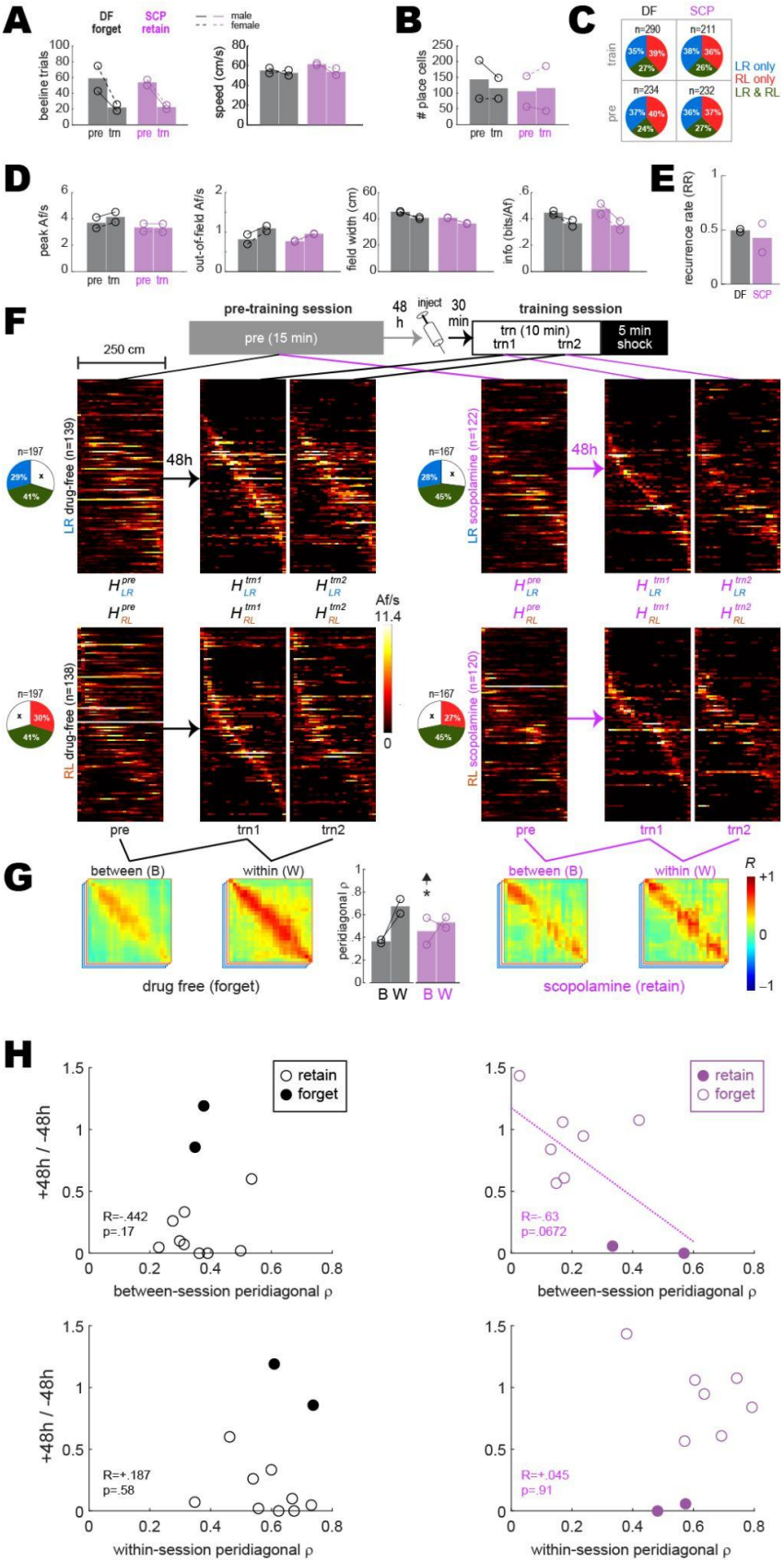

Supplementary Figure 5. *Pre-training and training session results from drug-free (DF) rats that failed to retain avoidance and scopolamine (SCP) rats that successfully retained avoidance.* Panels A-G are similar to those shown in panels C-I of Fig. 2 in Results, except here, results are shown for DF rats that failed to retain avoidance (n=2) and SCP rats that successfully retained avoidance (n=2) 48 h after training.The sample size of rats was not sufficient to perform ANOVAs, so independent t-tests were performed to compare values included in each graph bar against values in corresponding bars from Fig. 2 in Results. The only comparison to beat p<.05 (uncorrected) between-session peridiagonal ρ in the SCP condition ('*' and up arrow over center bar graph in panel G; compare with panel I of Fig. 2 in Results). Hence, in rats for which SCP failed to block avoidance, SCP also failed to impair between-session stability of place cell population vectors. Further supporting this conclusion, a marginally significant correlation was observed (see regression line in panel H, upper right) between 48 h avoidance retention scores and between-session peridiagonal ρ values in the SCP condition (n=11 rats, combining those that retained and forgot the avoidance response). Hence, lower between-session population vector stability was associated with more severely impaired retention of avoidance. No such correlations were observed in the DF condition or for within-session stability scores.

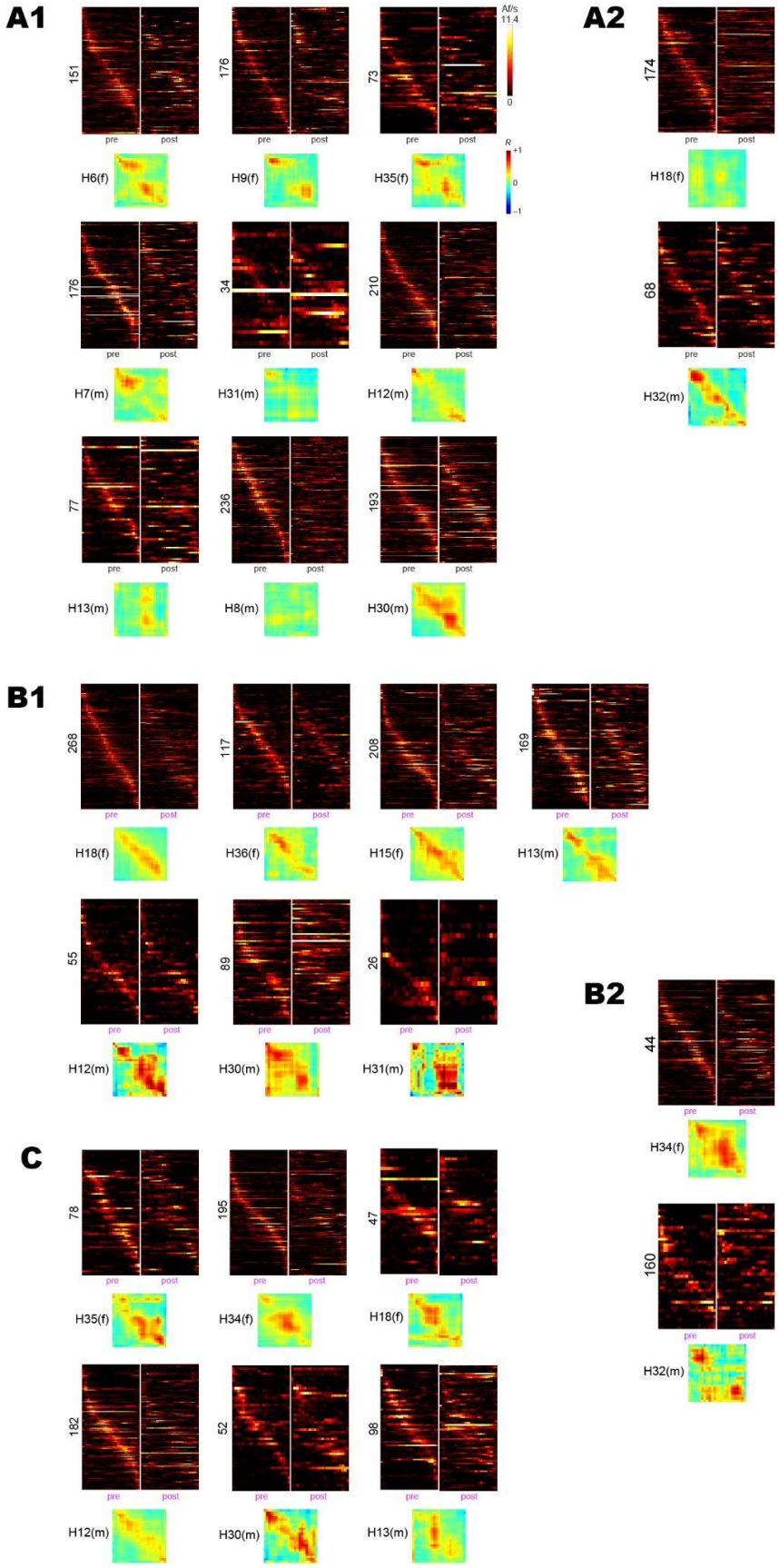

Supplementary Figure 6. *Pre-training and post- extinction session data from individual rats.* As in Fig. 3, heatmaps are shown for pre-training and post-extinction sessions, along with pre vs post population vector correlation matrices. *A1*) Rats (n=9) from the drug-free shock condition that showed 48 h avoidance retention. *A2*) Rats (n=2) from the drug-free shock condition that failed to show 48 h avoidance retention. *B1*) Rats (n=7) from the scopolamine condition that failed to show 48 h avoidance retention. *B2*) Rats (n=2) from the scopolamine shock condition that showed 48 h avoidance retention. *C*) Rats (n=6) from the barrier training control condition.

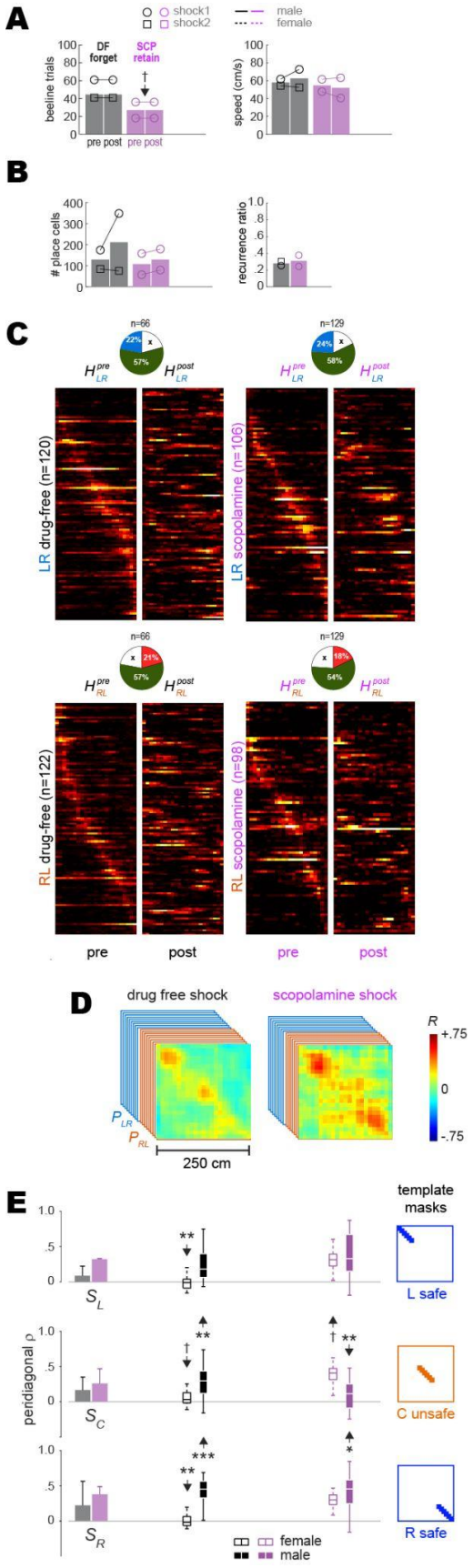

Supplementary Figure 7. *Pre-training and post-extinction results from drug-free (DF) rats that failed to retain avoidance and scopolamine (SCP) rats that successfully retained avoidance.* Panels A-E are similar to Fig. 3 panels B,C,D,F,G, respectively, in Results. Here, results are shown for DF rats that failed to retain avoidance (n=2) and SCP rats that successfully retained avoidance (n=2) 48 h after training. The sample size of rats was not sufficient to perform ANOVAs, so independent t-tests were performed to compare values included in each graph bar against values included in corresponding bars from Fig. 3. The number of beeline trials per session was equalized between sessions in each rat, but not between training conditions; beeline trial counts were marginally lower in SCP rats that retained avoidance responses (panel A, left graph) compared to those in Fig. 3 that failed to retain avoidance; this was because SCP rats that retained avoidance ran fewer beeline trials in the post extinction session (probably because they were expressing residual fear despite reaching the avoidance extinction criterion), resulting in a smaller equalized number of trials. Of the two DF rats that failed to retain avoidance, one appeared to show remapping and the other did not (see individual rat heatmaps in Supplementary Fig. 6, panel A2). Panel E shows that in the male DF rat that failed to retain avoidance or show remapping, peridiagonal ρ was significantly larger in the unsafe C zone and also in the safe R (but not L) zone compared with the mean from Fig. 3 for DF rats that retained avoidance (**p<.01, ***p<.001). Of the two SCP rats that retained avoidance, one appeared to show remapping of the unsafe center zone and the other did not (see individual rat heatmaps in Supplementary Fig. 6, panel B2). Panel E shows that in the male SCP rat that retained avoidance and showed remapping, peridiagonal ρ was significantly lower in the unsafe C zone (**p<.01 with down arrow), consistent with remapping of the shock zone.

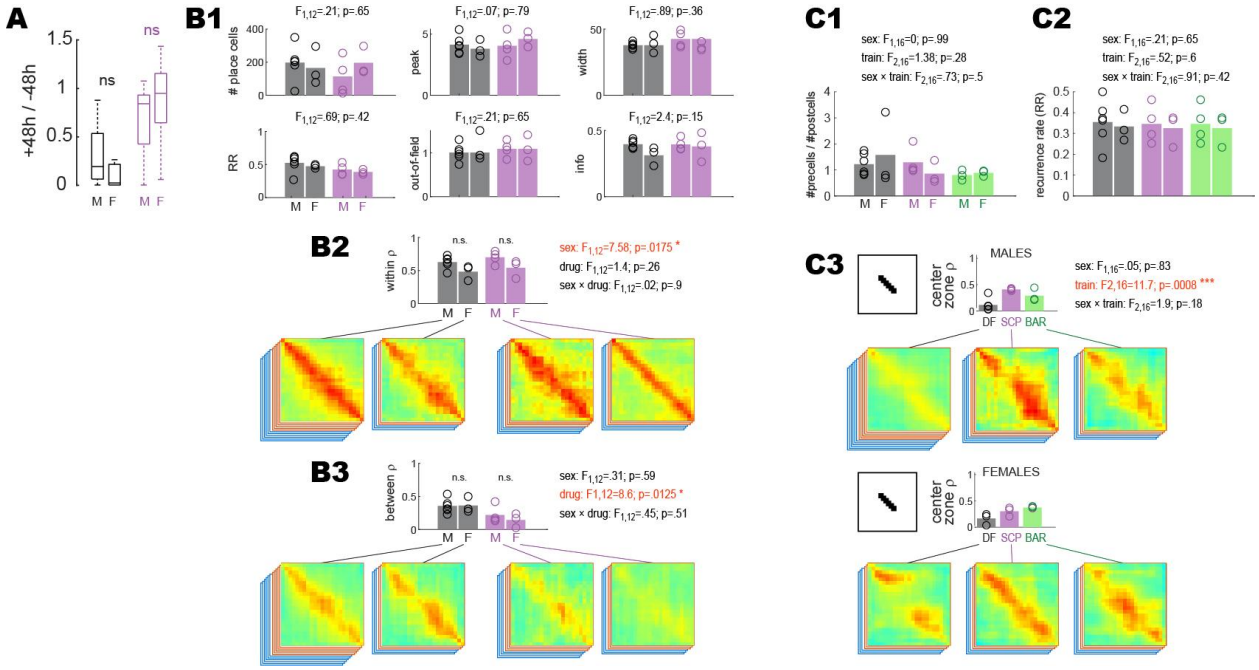

Supplementary Figure 8. *Avoidance and place coding in male versus female rats.* Statistical analyses were performed to compare results from male versus female rats. *A*) Mann-Whitney U tests found that 48 hour retention of avoidance behavior did not differ for males versus females in the drug-free or scopolamine shock conditions. *B*) 2x2 ANOVAs were performed with sex (M,F) and drug (drug-free, scopolamine) as independent factors. B1: There were no significant effects of sex upon the number of place cells imaged per rat (analysis shown for training session), recurrence ratio (RR), or spatial tuning properties (peak rate, out-of-field rate, field width, spatial information); main effect of sex is shown above each graph, however sex-by-drug interactions also were not significant (not shown). B2: As reported in the main text, there was no significant main effect of drug upon within-session population vector correlations, however there was a significant main effect of sex arising from the fact that females exhibited lower within-session population vector correlations than males in both drug conditions; this was the only significant effect of sex that was found in any of the analyses. B3: As reported in the main text, there was a significant main effect of drug upon between-session population vector correlations, however there was no significant main effect of sex and no sex-by-drug interaction. *C*) 3x2 ANOVAs were performed with sex (M,F) and training condition (DF,SCP,BAR) as independent factors. C1: The change in the number of imaged place cells between pre and post sessions (measured as the number of post session cells over the number of pre session cells) did not differ for males versus females; hence, neither sex showed a tendency to gain or lose more place cells than the other after avoidance acquisition and extinction. C2: Place cell recurrence rates (RR) between the pre and post sessions did not differ for males versus females. C3: Males and females showed similar learning-induced remapping in the center of the short path (black bars) and similar blockade of this remapping by scopolamine (pink bars).

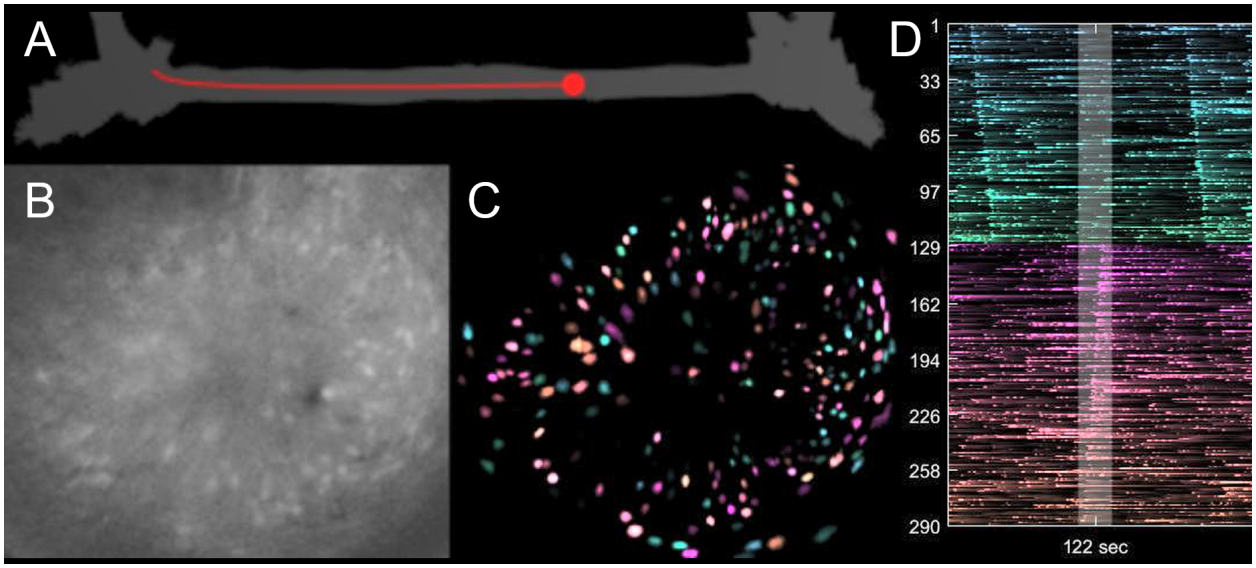

Supplementary Video 1 Video demonstrating behavior and calcium imaging recorded from one rat performing linear alternation along the short path of the maze A) position of the rat (red dot) B) Motion corrected video of calcium fluorescence C) Processed demixed/denoised CaImAn output (Spatial contours modulated by denoised calcium trace) D) Right half shows calcium activity of 290 identified neurons in the video, sorted by their preferred firing direction (teal/pink) and location along the track. Current time highlighted in center gray region.